

1 Leaf habit drives leaf nutrient resorption globally alongside nutrient 2 availability and climate

3 Gabriela Sophia^{1,2,3}, Silvia Caldararu⁴, Benjamin D. Stocker^{3,5}, Sönke Zaehle^{1,6}

4 [1] Max Planck for Biogeochemistry, Jena, Germany; [2] International Max Planck Research
5 School on Global Biogeochemical Cycles; [3] Geographisches Institut, Universität Bern,
6 Switzerland; [4] Discipline of Botany, School of Natural Sciences, Trinity College Dublin,
7 Dublin, Ireland; [5] Oeschger Center, Universität Bern, Switzerland; [6] Friedrich Schiller
8 Universität Jena, Jena, Germany; (gsophia@bgc-jena.mpg.de)

9

10 Abstract

11 Nutrient resorption from senescing leaves can significantly affect ecosystem nutrient cycling,
12 making it an essential process to better understand long-term plant productivity under
13 environmental change that affects the balance between nutrient availability and demand.
14 Although it is known that nutrient resorption rates vary strongly between different species
15 and across environmental gradients, the underlying driving factors are insufficiently
16 quantified. Here, we present an analysis of globally distributed observations of leaf nutrient
17 resorption to investigate the factors driving resorption efficiencies for nitrogen (NRE) and
18 phosphorus (PRE). Our results show that leaf structure and habit, together with indicators of
19 nutrient availability, are the two most important factors driving spatial variation in NRE.
20 Overall, we find higher NRE in deciduous plants ($65.2\% \pm 12.4\%$, $n=400$) than in evergreen
21 plants ($57.9\% \pm 11.4\%$, $n=551$), likely associated with a higher share of metabolic N in leaves
22 of deciduous plants. Tropical regions show the lowest resorption for N (NRE: $52.4\% \pm$
23 12.1%) and tundra ecosystems in polar regions show the highest (NRE: $69.6\% \pm 12.8\%$),
24 while the PRE is lowest in temperate regions ($57.8\% \pm 13.6\%$) and highest in boreal regions
25 ($67.3\% \pm 13.6\%$). Soil clay content, N and P atmospheric deposition - globally available
26 proxies for soil fertility - and mean annual precipitation (MAP) play an important role in this
27 pattern. The statistical relationships developed in this analysis indicate an important role of
28 leaf habit and type for nutrient cycling and guide improved representations of plant-internal
29 nutrient re-cycling and nutrient conservation strategies in vegetation models.

30 **Keywords:** Leaf nutrient content; Leaf structure; Nitrogen and phosphorus resorption
31 efficiency; Plant ecophysiology; Plant functional traits; Plant nutrient limitation.

33 **1. Introduction**

34 Nutrient cycling plays an important role in shaping the global distribution of terrestrial
35 primary productivity (LeBauer et al., 2008; Zaehle, 2013; Du et al., 2020). Nitrogen (N) and
36 phosphorus (P) are the main limiting nutrients for plant growth. N is needed to maintain and
37 produce essential proteins for the biosynthesis; while P is an element of genetic material and
38 plays a major role in the regeneration of the main receptor of carbon (C) assimilation, and in
39 the production of energy that conducts many processes in living cells (Chapin, 1980;
40 Güsewell, 2004). The anthropogenic increase in atmospheric CO₂ since the beginning of
41 industrialization has the potential to enhance the terrestrial carbon sink through increasing
42 plant photosynthetic rates, a process known as CO₂ fertilization (Bazzaz, 1990). A potential
43 limitation to the fertilization effect is progressive nutrient limitation to growth (Luo et al.,
44 2004) and associated plant strategies to deal with such limitations. Thus, understanding the
45 ways in which nutrients circulate in ecosystems and are acquired, lost, and conserved by
46 plants, is essential for simulating plant response to global changes.

47 Nutrient resorption - defined here as the translocation of nutrients from senescing leaves to
48 temporary storage tissues - is a plant strategy for nutrient conservation (Killingbeck, 1996;
49 Kobe et al., 2005). It allows plants to directly reuse nutrients, decreasing the dependence on
50 soil nutrient availability and the competition for these nutrients with other plants and
51 microbes, especially in nutrient-limited environments (Aerts, 1996; Aerts and Chapin, 1999).
52 The question that arises is then why do plants not all resorb the entirety of leaf nutrients for
53 being more efficient? The fact that they do not achieve their maximum resorption capacity
54 implies the existence of costs and limitations to resorption. A quantitative understanding of
55 nutrient resorption can yield insights into plant strategies to cope with nutrient limitation
56 (Aerts and Chapin, 1999; Chapin et al., 2011). This is because the resorption process
57 influences most other ecosystem processes that determine plant growth, as it directly affects
58 litter quality and therefore soil organic matter decomposition and has indirect consequences
59 for plant nutrient uptake, carbon cycling and finally plant competition (Killingbeck, 1996;
60 Berg and McClaugherty, 2008). The average fraction of leaf nutrients resorbed before
61 abscission is estimated to be ~62% for N and ~65% for P (Vergutz et al., 2012). Cleveland et

62 al. (2013) estimated that this corresponds to 31% of a plant's annual demand for N and 40%
63 of the annual demand for P, but with large geographical and species variations.

64 However, despite advances in recent years, the drivers behind nutrient resorption and its
65 variation are still unclear: First, soil fertility has long been assumed to be a key driver for
66 variations in nutrient resorption, with increased resorption in infertile soils as the plant's main
67 strategy for nutrient conservation (Aerts and Chapin, 1999). This interpretation has also
68 provided a basis for modeling dynamic resorption efficiency by accounting for nutrient
69 availability in global vegetation models (Fisher et al., 2010; Lawrence et al., 2019).
70 Nonetheless, there is diverging evidence established at different geographic scales, showing
71 positive correlations (Aerts and Chapin, 1999), negative correlations (Yuan and Chen, 2015;
72 Xu et al., 2021), and even a lack of correlation between soil fertility and resorption efficiency
73 (Vergutz et al., 2012). Second, climate factors are also considered to be important drivers for
74 resorption, but the evidence is equally conflicting: On the one hand, Yuan and Chen (2009)
75 and Yan et al. (2018) suggested nitrogen resorption efficiency (NRE) is decreasing with mean
76 annual temperature (MAT) and precipitation (MAP), with the opposite trend for phosphorus
77 resorption efficiency (PRE), arguing that colder regions tend to be more N-limited, while
78 P-limitation is observed more commonly in warmer environments. From low to high latitudes
79 globally, the role of N in limiting productivity tends to increase as the availability of N is
80 mainly determined by temperature-limited processes such as biological N fixation and
81 mineralization of soil organic matter (Cleveland et al., 2013; Fay et al., 2015; Deng et al.,
82 2018), but the presence of N fixers in tropical forests introduces complexity to the pattern of
83 nutrient limitation between tropical and temperate zones (Hedin et al., 2009). Nevertheless,
84 the limited availability of P in the tropics due to highly weathered soils distinguishes low- to
85 mid-latitude environments (Elser et al., 2007). On the other hand, Vergutz et al. (2012) and
86 Xu et al., 2021 showed that NRE and PRE are both increasing with decreasing MAT and
87 MAP toward higher latitudes.

88 A third set of studies suggests plant functional types (PFTs), leaf stoichiometry and plant
89 nutrient demand as drivers for nutrient resorption (Reed et al., 2012; Han et al., 2013; Tang et
90 al., 2013; Brant and Chen, 2015; Du et al., 2020; Chen et al., 2021a; Sun et al., 2023). When
91 found greater nutrient resorption in evergreen species, it is assumed to be a conservation
92 strategy given their comparatively low leaf nutrient content and slow growth rate and
93 predominant occurrence in nutrient-limited biomes (Killingbeck, 1996; Yan et al., 2018; Xu

94 et al., 2021). The same argument has been used for interpreting differences between
95 broad-leaves and needle-leaves, in which nutrient resorption is generally observed to be
96 higher in needles as a strategy to acclimatize and survive in resource-limited environments
97 (Aerts and Chapin, 1999; Yuan et al., 2005; Yan et al., 2018; Xu et al., 2021). Previous
98 studies have suggested that shrub species generally display higher nutrient resorption rates
99 compared to trees, due to their smaller leaves with shorter life cycles and for the need to
100 optimize nutrient use in resource-limited environments (Killingbeck, 1996; Yuan and Chen,
101 2009; Yan et al., 2018; Xu et al., 2021). However, Brant and Chen (2015) suggest that
102 deciduous plants are more dependent on nutrient resorption as their investment in green leaf
103 nutrients is higher to maintain their fast growth through high physiological activity during the
104 growing season. Plants with a slow growth strategy, such as evergreens and needle-leaves,
105 have lower photosynthetic nutrient use efficiency due to a higher allocation of C and N to leaf
106 structural rather than metabolic compounds (Reich et al., 2017). Onoda et al. (2017)
107 empirically supports this by showing that a greater allocation of nutrients to structural
108 compounds is associated with decreased specific leaf area (SLA) and increased diffusive
109 limitation to photosynthesis. Thus, variations in leaf traits and construction costs could
110 contribute to differences in resorption between PFTs. Nevertheless, Drenovsky et al. (2010;
111 2019) suggested that resorption variability is influenced by an interplay of the discussed
112 drivers, that includes soil properties, climatic conditions, and plant characteristics. Estiarte et
113 al. (2023) support that leaf biochemistry of plants determine the first limitation to nutrient
114 resorption, with a secondary regulation in resorption by environmental conditions, while the
115 costs of leaf aging remain consistent.

116 The divergence of observed patterns highlights the need for further investigation into the
117 main drivers of variations in nutrient resorption, distinguishing the influence of plant types,
118 soil and climatic conditions. In this study, we present a meta-analysis that combines the
119 version 5.0 of TRY Plant Trait database (Kattge et al., 2020) with different ancillary datasets
120 for climate and soil factors to investigate global patterns of resorption efficiencies for N and
121 P. We aim to extend woody species observations for nutrient resorption and investigate the
122 factors that explain observed patterns along three main axes: climate, soil fertility and leaf
123 properties.

124

125

126 2. Methods

127 2.1 Data collection

128 We assembled the dataset from the TRY Plant Trait database (<https://www.try-db.org>, Kattge
129 et al., 2020, version 5.0) containing field measurements of paired leaf and litter mass-based
130 tissue N and P concentrations ($N_{\text{mass, leaf}}$, $P_{\text{mass, leaf}}$, $N_{\text{mass, litter}}$, $P_{\text{mass, litter}}$) to derive the fractional
131 nutrient resorption (described in Sect. 2.2), and plant functional traits recorded in parallel
132 from the same species and same location to consider as biological predictors variables (Table
133 1). As additional predictors for nutrient resorption, we combined it with climate and soil input
134 data (Table 2). We processed the data using R statistical software (version 4.0.4), keeping the
135 data at species-level. To manipulate the extracted functional traits, we used the package
136 {rtry} (Lam et al., 2022) developed to support the preprocessing of TRY Database (version
137 1.0.0), and {tidyverse} package (Wickham et al., 2019) with its dependencies (version 1.3.2).
138 The data processing followed the quality control according to the published protocol of TRY
139 (Kattge et al., 2011; 2020).

140

141 **Table 1.** Traits extracted from TRY database to derive nutrient resorption.

Plant traits	Variable name	Unit
$N_{\text{mass, leaf}}$	Leaf nitrogen (N) content per leaf dry mass	mg g
$P_{\text{mass, leaf}}$	Leaf phosphorus (P) content per leaf dry mass	mg g
$N_{\text{mass, litter}}$	Litter nitrogen (N) content per litter dry mass	mg g
$P_{\text{mass, litter}}$	Litter phosphorus (P) content per litter dry mass	mg g
SLA	Specific leaf area with different structural exclusions: - Petiole, rachis and midrib excluded - Petiole excluded - Petiole included - Undefined if petiole is in- or excluded	mm ² mg ⁻¹
LDM	Leaf dry mass	mg
LDM _{senes}	Leaf senescent dry mass	mg
LML	Leaf mass loss	unitless
PFT	Plant functional type / growth form	unitless
KGC	Köppen climate classification	unitless

142

143

144 As predictors, we used a set of climate variables, N and P deposition, vegetation type-related
145 variables, and soil data (Table 2) with a spatial resolution of 0.5° × 0.5° to match that of the

146 lowest resolution dataset (P deposition). Soil fertility was represented here by N and P
 147 deposition and other soil characteristics that globally correlate with nutrient availability, such
 148 as total soil P and soil texture. MAT, MAP and seasonal temperature amplitude were derived
 149 from the global climate database WorldClim (Fick and Hijmans, 2017). We extracted the
 150 Köppen climate classification to represent different climate zones from the TRY database and
 151 filled data gaps using the {Kgc} R package (Bryant et al., 2017), which provides the Köppen
 152 climate classification for each latitude and longitude. We calculated mean annual
 153 evapotranspiration (ET) and growing season length (GSL) from FLUXCOM (Jung et al.,
 154 2011), in which GSL was based on the seasonal phasing of gross primary productivity (GPP)
 155 considering the time period between 20% and 80% of maximum GPP in an average year for
 156 the period 2002-2015. Total soil P concentrations were derived from Yang et al. 2013; soil
 157 clay content and soil pH were extracted from the Harmonized World Soil Database (HWSD;
 158 Wieder et al., 2014). We used atmospheric N deposition values from CESM-CMIP6 (Hegglin
 159 et al., 2016) taking the year 2010 as a reference, summing the emissions and making the
 160 annual mean; and P deposition was extracted from Brahney et al. (2015) and Chien et al.
 161 (2016). The N deposition data is interpolated to annual from decadal time-slices and derived
 162 from initialized CAM runs, therefore, the information contained is representative of
 163 large-scale features. For consistency with P deposition, where we only have a decadal mean
 164 estimate, we chose not to include the trend information. All variables used as predictors of
 165 global N and P resorption are described in table 2.

166

167 **Table 2.** All possible predictors for nutrient resorption.

	Variable name	Unit	Reference
MAT	Mean annual temperature	°C	Fick and Hijmans, 2017
MAP	Mean annual precipitation	mm	Fick and Hijmans, 2017
AmplT	Temperature amplitude	°C	Fick and Hijmans, 2017
ET	Evapotranspiration	mm	Jung et al., 2011
N_dep2010	Nitrogen deposition	kgN ha yr	Hegglin et al., 2016
P_dep	Phosphorus deposition	kgN ha yr	Brahney et al., 2015; Chien et al., 2016

soilP_tot	Total soil P	g P/m ²	Yang et al., 2013
Clay	Top soil clay content	% weight	Wieder et al., 2014
pH	Top soil pH	-log(H ⁺)	Wieder et al., 2014
GSL	Growing season length	days	Jung et al., 2011
SLA	Specific leaf area	mm ² mg ⁻¹	Kattge et al., 2020
LLS	Leaf Longevity	month	Kattge et al., 2020
Leaf habit	Deciduous/Evergreen	-	Kattge et al., 2020
Leaf Type	Broadleaves/Needles	-	Kattge et al., 2020

168

169

170 2.2 Data derivation

171 We defined nutrient resorption efficiency (NuRE) as the amount of nutrient resorbed during
172 leaf senescence calculated as:

173

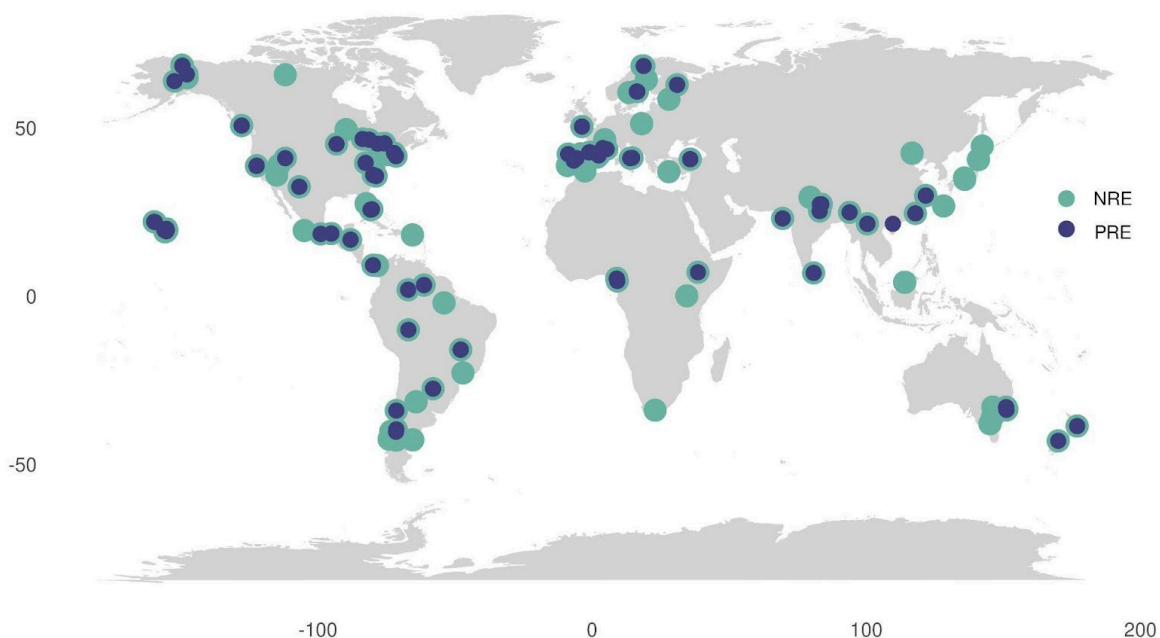
$$174 \quad NuRE = \left(1 - \frac{Nu_{senesced}}{Nu_{green}} MLCF\right) \times 100 \quad (1)$$

175

176 where Nu_{green} and $Nu_{senesced}$ are nutrient (N or P) concentrations in dry green and senesced
177 leaves (mg g), respectively; MLCF (unitless) is the mass loss correction factor during
178 senescence to account for the loss of leaf mass when senescence occurs. Omitting MLCF
179 overestimates nutrient concentration in senescent leaves and underestimates resorption values
180 (Zhang et al., 2022). Zhang et al. (2022) showed a significant overall improvement when
181 considering MLCF, where both average of N and P resorption increased by ~9%, particularly
182 for cases with low resorption efficiencies. In the present study, not considering the MLCF
183 also underestimates the actual nutrient resorption efficiency when comparing the fraction of
184 resorption of four sub datasets from the final global dataset (Appendix A).

185 We calculated MLCF as the ratio between the dry mass of senesced and green leaves (Van
186 Heerwaarden et al., 2003a), where it was not directly available as percentage leaf mass loss

187 (LML) in the data. We derived average values of MLCF per plant type from nutrient
188 resorption dataset to fill missing values: 0.712 for deciduous, 0.766 for evergreen, 0.69 for
189 conifers, and 0.75 for woody lianas, respectively. To fill in MLCF values for the remaining
190 leaf nutrient and litter data from TRY, we associated these means of MLCF with leaf habit,
191 leaf type and growth form information available on each species. For that, trees with needle
192 evergreen leaves were associated with conifers MLCF; deciduous trees/shrubs with
193 deciduous woody MLCF, and evergreen trees/shrubs with evergreen woody MLCF,
194 respectively. We grouped climbers and lianas with shrubs. Initially, 107 observations for NRE
195 and 76 observations for PRE were derived from site-level MLCF data. We increased these
196 numbers by 847 for NRE and 378 for PRE when applying the mean MLCF per PFT. In total
197 we extracted data from 131 sites for NRE and 74 for PRE (Fig. 1), with more than one entry
198 per site giving a total of 954 and 454 data points for NRE and PRE species-level,
199 respectively. Temperate biomes were most strongly represented in the dataset (518 entries),
200 followed by tropical (180), boreal (103), polar (102) and dry ecosystems (65).



201

202 **Figure 1:** Global distribution of data for nitrogen resorption efficiency (NRE) and phosphorus
203 resorption efficiency (PRE). Data includes observations from 131 sites for NRE (green circles) and 74 sites for PRE (blue
204 circles). Each site may have multiple entries, resulting in a total of 954 NRE data points and 454 PRE data
205 points at the species level.

206

207

208

209 2.3 Statistical analysis

210 As the nutrient resorption data did not conform to a normal distribution (Shapiro–Wilk test),
211 we used the nonparametric Kruskal–Wallis one-way ANOVA test of variance to examine
212 differences of NRE and PRE among different climate zones, and Mann-Whitney Wilcoxon
213 test to evaluate differences between leaf habit, leaf type and growth form (deciduous vs
214 evergreen plants, broad-leaves vs needle-leaves, shrubs vs trees), using the {ggstatsplot} R
215 package (Patil, 2021). We applied Pearson correlation and linear regression to analyze the
216 relationship between nutrient resorption and the predictors described in Table 2. For MAP
217 and N deposition, we performed a log transformation prior to conducting the analysis to have
218 the distribution close to the normal. To find the best set of predictors for the variance in NRE
219 and PRE, we used multimodel inference (MMI; Burnham and Anderson, 2002) using the
220 Akaike’s information criterion (AIC) and estimated the relative importance of each
221 explanatory variable. Different from setting only a single model based on AIC, multimodel
222 inference accounts for uncertainties in the model performance and in the considered
223 parameters. This approach involves modeling and evaluating all possible combinations of a
224 predetermined set of predictors. The evaluation is typically conducted using a criterion, such
225 as AIC or Bayesian information criterion (BIC), which favors simpler models and allows for
226 a comprehensive examination of all possible models and their respective performances. By
227 synthesizing the estimated coefficients of predictors across these models, MMI enables
228 inference regarding the overall importance of specific predictors. Before applying MMI, we
229 used generalized linear mixed effect models (GLMER) to fit different models after removing
230 drivers described in Table 2 that showed: (1) high collinearity between them ($R \geq 0.7$; Fig.
231 S5); (2) non-significant correlation with NRE (soil P) and PRE (MAP and SLA) (Fig. S5);
232 (3) a threshold of Variance Inflation Factor (VIF) higher than 10 (James et al., 2013).
233 Specifically, temperature amplitude, GSL and ET were not considered due to their high
234 correlation with MAT and MAP and due to high VIF. Based on ecological interactions, we
235 fitted the model considering interactions between climate variables MAT and MAP, as well as
236 between plant characteristics such as leaf structure, leaf habit and leaf type
237 (SLA:LeafHabit:LeafType). We accounted for species identity as a random factor in the
238 mixed effect models to test if intrinsic intra-specific variability plays a role. Environmental
239 and biotic factors have strong shared effects in linear mixed models and therefore are not
240 assessed separately in this study. If the ratio between the sample size and the number of

241 parameters considered was higher than 40, we fitted the model using Restricted Maximum
242 Likelihood REML and AICc (corrected for small sample sizes) to avoid bias. We selected the
243 model with lowest AIC and applied it into the ‘dredge’ function implemented in the
244 multimodal inference package {MuMIn} (Bartoń K, 2023) which generated a full submodel
245 set. A set of best-performing models for NRE and PRE was selected using a cut-off of ΔAIC
246 < 2 , and based on these top models, the best model parameters were generated. Using
247 {MuMIn} package, we also calculated the relative importance of each predictor through the
248 sum of the Akaike weights across all models in which the respective parameter was being
249 considered, with a cut-off of 0.8 to distinguish between important and unimportant predictors
250 (Terrer et al., 2016). The marginal and conditional R^2 values for the fitted mixed models were
251 0.23 and 0.98 for NRE, and 0.29 and 0.48 for PRE respectively, therefore, fixed and random
252 effects explain 98% of the variance in NRE and 48% in PRE, with fixed effects alone
253 explaining 23% for NRE and 29% for PRE. We performed all statistical analysis using
254 p-value < 0.05 as statistically significant.

255

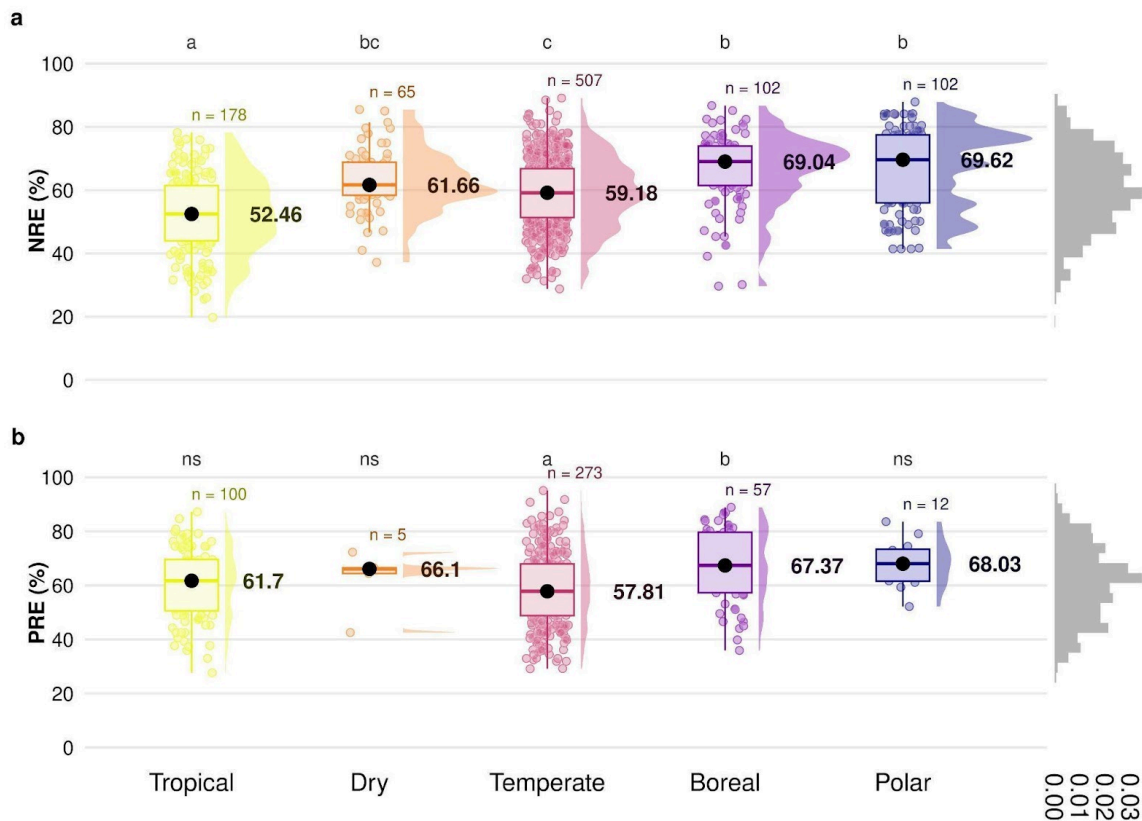
256

257 3. Results

258 3.1 Global patterns of nutrient resorption between different climate zones

259 The global median of nutrient resorption is 60.0% for N \pm 12.3% of standard deviation
260 (n=954) and 61.2% for P \pm 13.6% (n=454), respectively. We find differences for both NRE
261 and PRE between the climate zones (Fig. 2). Tropical regions show the lowest resorption for
262 N (NRE: 52.4% \pm 12.1%) and tundra ecosystems in polar regions show the highest (NRE:
263 69.6% \pm 12.8%) (Fig. 2a). PRE in temperate regions shows the lowest values (57.8% \pm
264 13.6%). PRE increases towards the higher latitude with significant difference of P resorption
265 from temperate to boreal regions (67.3% \pm 13.6%) (Fig. 2b). In contrast to NRE, the
266 difference of PRE between tropical and other climate zones, as well as polar regions, is not
267 statistically significant ($P > 0.05$). NRE in dry regions (61.6% \pm 9.7%) is statistically
268 different from tropical and polar regions, while for PRE, the difference is not significant
269 between climate zones. However, the sample for this zone is substantially smaller. Details of
270 minimum, maximum, and median values can be found in Table B1.

271



272

273 **Figure 2:** Difference in nitrogen resorption efficiency (NRE %) and phosphorus resorption efficiency (PRE %) among climate gradients from tropical to polar zones based on the Köppen climate classification. Panels display NRE (a) and PRE (b), with boxplots showing the median (black dots), interquartile range and outliers, indicating data spread and variability. The side distributions show the overall data distribution for each climate zone. Different letters indicate statistically significant differences in nutrient resorption efficiency between climate zones. 'ns' indicates no significant difference. 'n' represents the number of observations per climate zone. The gray distribution on the right of each panel represents the overall distribution of NRE and PRE values across all observations.

281

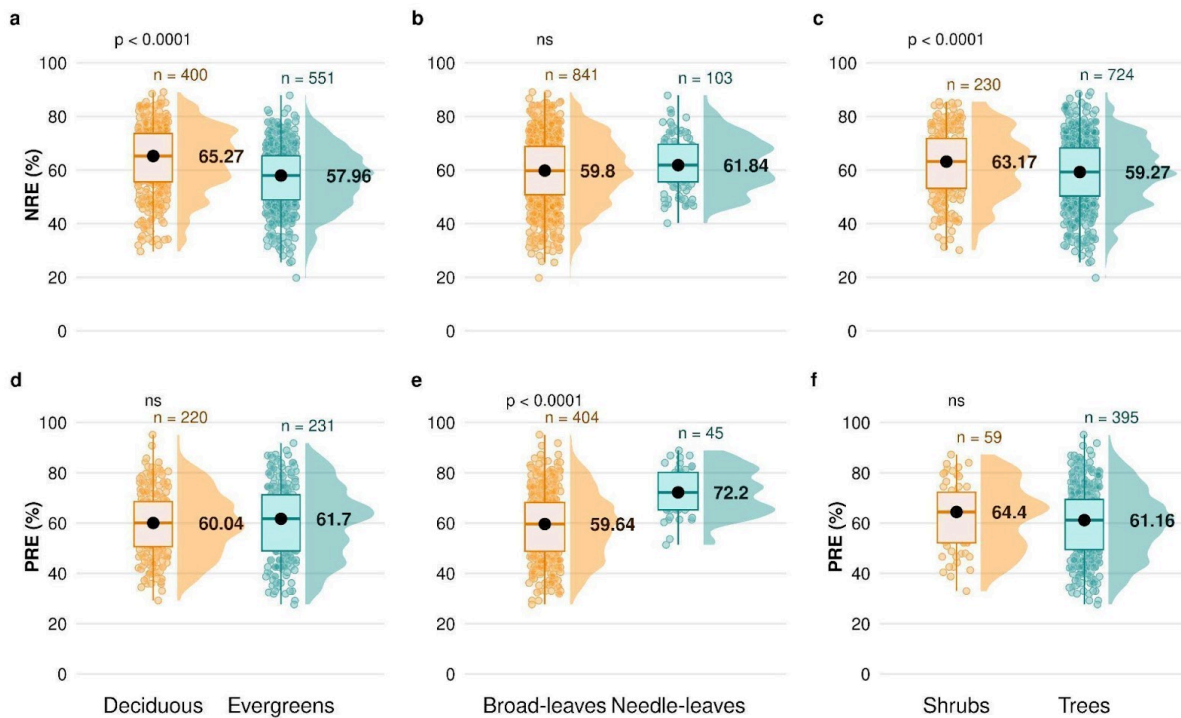
282

283 3.2 Patterns of nutrient resorption between plant functional types

284 We explore the variation of nutrient resorption between plant functional groups. Deciduous woody plants have a significantly higher NRE ($65.2\% \pm 12.4\%$, $n=400$) than evergreens ($57.9\% \pm 11.4\%$, $n=551$) ($P < 0.001$) (Fig. 3a), and shrubs have a significantly higher NRE ($63.1\% \pm 12.4\%$, $n=230$) than trees ($59.2\% \pm 12.1\%$, $n=724$) ($P < 0.001$) (Fig. 3c). Conversely, there is no significant difference in NRE between broad- ($59.8\% \pm 12.5\%$, $n=841$) and needle-leaved plants ($61.8\% \pm 9.9\%$, $n=103$) ($P > 0.05$) (Fig. 3b). PRE does neither differ significantly between deciduous ($60.0\% \pm 12.8\%$, $n=220$) and evergreen plants ($61.7\% \pm 14.4\%$, $n=231$) ($P = 0.4$) (Fig. 3d) nor between shrubs ($64.4\% \pm 13.5\%$, $n=59$) and trees ($61.1\% \pm 13.6\%$, $n=395$) ($P = 0.2$) (Fig. 3f). However, PRE differs significantly between leaf types, with needle-leaved showing higher resorption ($72.2\% \pm 9.2\%$, $n=45$) than

294 broad-leaved plants ($59.6\% \pm 13.5\%$, $n=404$) ($P < 0.001$) (Fig. 3e). Details of minimum,
 295 maximum and median values can be found in Table B2.

296



297

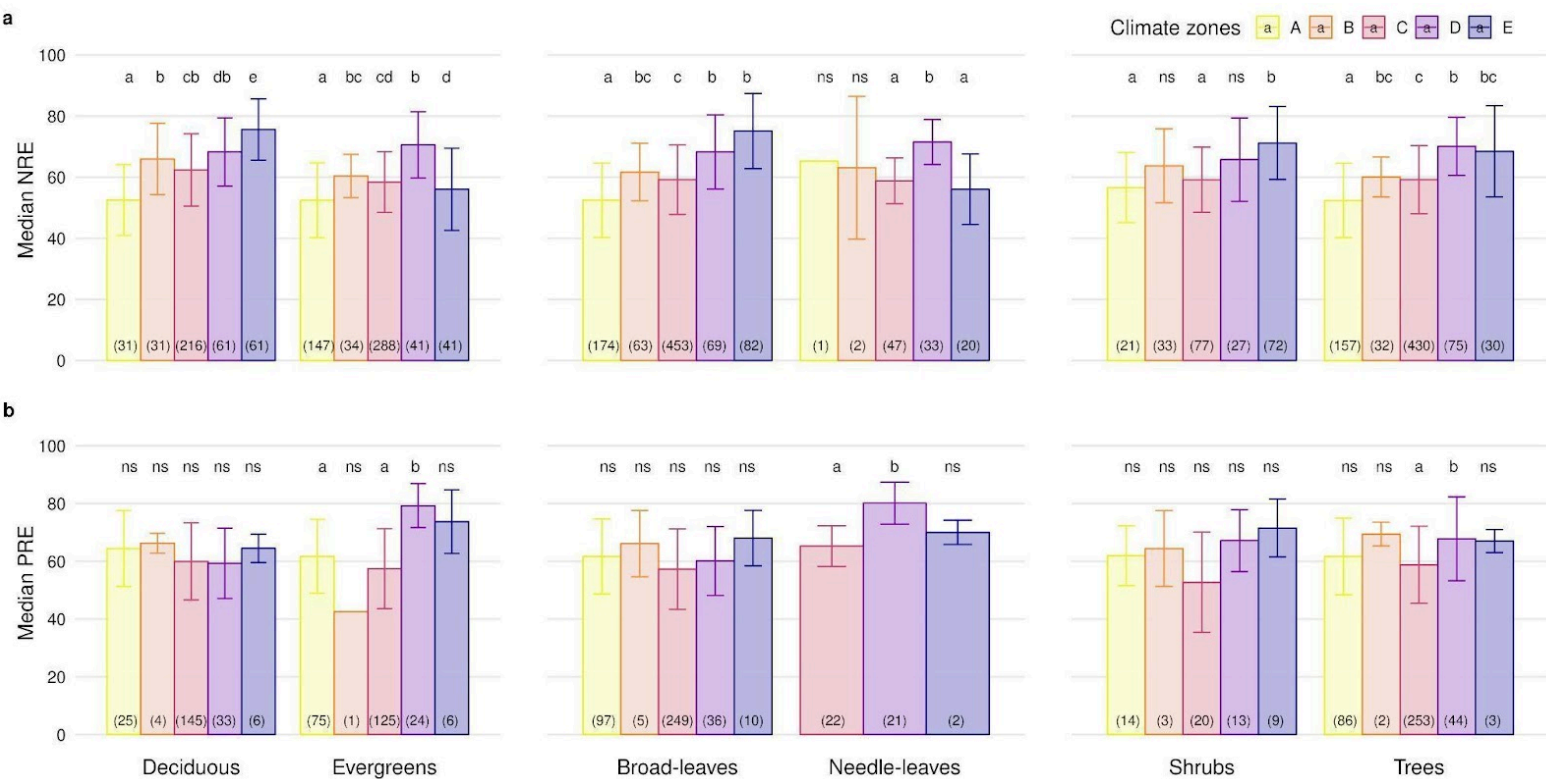
298 **Figure 3:** Differences in nitrogen resorption efficiency (NRE %) and phosphorus resorption efficiency (PRE %)
 299 between plant functional types (PFTs) on a global scale. Panels display NRE (a, b, c) and PRE (d, e, f) for
 300 different PFT comparisons: deciduous vs. evergreen species (a, d), broad-leaved vs. needle-leaved species (b,
 301 e), and shrubs vs. trees (c, f). Boxplots depict median (black dots), interquartile range and outliers, indicating
 302 data spread and variability. The side distributions show the overall data distribution for each PFT. ‘n’ represents
 303 the number of observations, ‘p’ values indicate the significance of differences in nutrient resorption efficiency
 304 between PFTs, and ‘ns’ indicates no significant difference.

305

306 We next explore how climate zones affect NRE and PRE within plant functional groups. NRE
 307 tends to increase from tropical to boreal climates (Fig. 4a) – a pattern seen among deciduous
 308 and evergreen woody plants, among shrubs and trees, and among broadleaved, but not
 309 needle-leaved plants. Also PRE increases from temperate to boreal and polar climates, but
 310 declines from the tropics to temperate climates in evergreens (Fig. 4b). Apart from the overall
 311 tendency, we observe a few statistical deviations from the general pattern that emerges across
 312 all plants pooled: NRE is significantly lower in polar regions compared to boreal forests for
 313 evergreens (NRE: $56.0\% \pm 13.4\%$; NRE: $70.5\% \pm 10.8\%$) and compared to needle leaved
 314 plants (NRE: $56.0\% \pm 11.5\%$; NRE: $51.5\% \pm 7.3\%$) ($P < 0.001$); PRE shows the same pattern
 315 deviation between these regions, but the pattern is not statistically significant ($P > 0.05$).
 316 Also, we do not observe lower NRE for tropical regions in needle leaved plants because the

317 only observation of this plant type is in this climate zone. Details of minimum, maximum and
 318 median values can be found in Table B3.

319



321 **Figure 4:** Median nitrogen resorption efficiency (NRE %) and phosphorus resorption efficiency (PRE %) across
 322 different plant functional types (PFTs) and climate zones. Panels display median NRE (a) and PRE (b) for the
 323 following PFTs: deciduous vs. evergreen species, broad-leaved vs. needle-leaved species, and shrubs vs. trees.
 324 Each bar represents a climate zone (A Tropical; B Dry; C Temperate; D Boreal; E Polar) based on the Köppen
 325 classification, with color-coded legends. Error bars indicate variability. Numbers in parentheses denote the
 326 number of observations and letters above bars indicate statistically significant differences between climate zones
 327 within each PFT. 'ns' indicates no significant difference).

328

329

330 3.3 Main drivers of nutrient resorption

331 We investigate the main drivers for variation in nutrient resorption, considering biological,
 332 climatic, and soil factors and using data from all PFTs and climate zones pooled. Dredge
 333 model averaging based on a set of best-performing models with corrected AIC (see Methods
 334 2.3) shows that the best model for NRE includes soil clay content, N deposition, MAP and
 335 growth form (Table 3). The best combination of predictors for the PRE model includes N
 336 deposition, leaf type, and MAT (Table 3). Sums of Akaike weights indicate that the order of
 337 importance of predictors for NRE is N deposition (RI 0.99), MAP (RI 0.99), leaf habit (RI
 338 0.98), followed by soil clay content (RI 0.97), growth form (RI 0.93) and leaf type (RI 0.87)

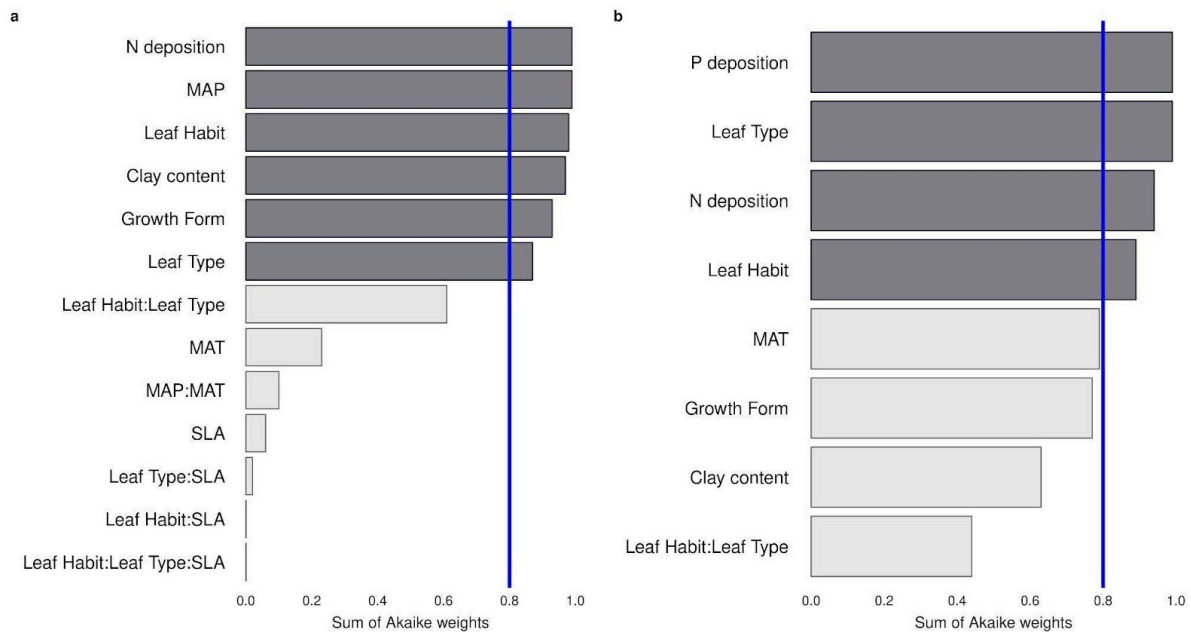
339 (Fig. 5a); while for PRE, the order is P deposition (RI 0.99), leaf type (RI 0.99), N deposition
 340 (RI 0.94) followed by leaf habit (RI 0.89) (Fig. 5b). The criteria to fit the model selecting
 341 and/or excluding predictors and interactions for the multimodel inference can be found in
 342 Sect. 2.3. Correlations between all variables, as well as linear relationships with the
 343 regression slope between nutrient resorption and all possible predictors can be found in Figs.
 344 C1 and C2.

345

346 **Table 3** | Summarized results of dredge model averaging for nitrogen resorption efficiency (NRE) and
 347 phosphorus resorption efficiency (PRE). Significant codes: 0 '****' 0.001 '**' 0.01 '*' 0.05 '.' 0.1 ' ' 1. SE
 348 means standard error.

NRE	Estimate	SE	Adjusted SE	z value	Pr(> z)
(Intercept)	63.24	2.86	2.87	21.96	<0.001 ***
Clay content	-0.33	0.09	0.09	3.54	<0.001 ***
Growth Form	2.57	1.11	1.12	2.30	0.02 *
Leaf habit	2.02	2.32	2.33	0.86	0.38
Leaf type	0.66	2.51	2.52	0.26	0.79
MAP	-5.07	1.58	1.58	3.19	0.001 **
N deposition	0.57	0.11	0.11	5.07	<0.001 ***
Leaf habit:Leaf type	-0.51	2.69	2.70	0.19	0.84
PRE	Estimate	SE	Adjusted SE	z value	Pr(> z)
(Intercept)	78.28	9.45	9.56	8.18	<0.001 ***
Clay content	-0.44	0.24	0.24	1.81	0.06 .
Growth Form	-1.35	2.99	3.03	0.44	0.65
Leaf habit	2.72	1.75	1.77	1.53	0.12
Leaf type	-10.34	4.29	4.35	2.37	0.01 *
MAT	1.08	0.49	0.49	2.18	0.02 *
N deposition	-1.77	0.54	0.54	3.23	0.001 **
P deposition	-97.13	65.80	66.75	1.45	0.14

349



350

351 **Figure 5:** Importance of the abiotic and biotic predictors on nitrogen resorption efficiency (NRE; **(a)** and
 352 phosphorus resorption efficiency (PRE; **(b)**). The relative importance (RI) of each predictor is calculated
 353 through the sum of the Akaike weights derived from multimodal inference selection, using corrected Akaike's
 354 information criteria. The blue line marks the threshold for important predictors (RI > 0.8). Interactions between
 355 predictors are denoted by colons. Mean Annual Precipitation (MAP); Mean Annual Temperature (MAT); SLA
 356 (Specific Leaf Area).

357

358

359 4. Discussion

360 Through an extensive global dataset of leaf nutrient resorption and a multifactorial analysis,
 361 we show that leaf habit and type are a strong driver of the spatial variation in nutrient
 362 resorption, with thicker, longer-lived leaves having lower resorption efficiencies. Climate,
 363 and soil-availability-related factors also emerge as strong drivers, in which we discuss a
 364 secondary regulation related to environmental conditions in space and time. Our study covers
 365 significantly more woody species observations for nutrient resorption, especially for N, than
 366 previous studies (Yuan and Chen, 2009; Yan et al., 2018; Xu et al., 2021). We also account
 367 for variations in the mass loss of senescing leaves by deriving the MLCF when leaf mass loss
 368 or leaf dry mass were available, and then apply the calculated average MLCF to the missing
 369 data, rather than using a single average of MLCF from the literature per PFT (Yan et al.,
 370 2018; Xu et al., 2021), which may lead to a more correct estimate of nutrient resorption (see
 371 Methods 2.2).

372

373 4.1 Nutrient resorption limited by leaf structure

374 The structural properties of leaves limit the efficiency of resorption along geographic and
375 climatic ranges. We find that the global median for NRE is significantly higher in deciduous
376 than evergreen plants, and is higher in shrubs than trees (discussed at the end of this section)
377 (Fig. 3a; 3c). This finding is in contrast to previous global studies that found decreasing
378 nutrient resorption with increasing green leaf nutrient content, implying that deciduous
379 species, which generally have higher leaf N content than evergreen species, have lower
380 resorption (Yan et al., 2018; Xu et al., 2021). Nevertheless, our finding is in agreement with
381 Vergutz et al (2012), who reported that deciduous woody species had higher NRE than
382 evergreen woody species and who found no significant differences for PRE.

383 We find that leaf habit is a strong driver for variation in resorption for both nutrients (Table 3;
384 Fig. 5). Fig. 3a shows that leaf habit is associated with clearly different median NRE values
385 for evergreen and deciduous species, while the relationship of the average resorption is less
386 clear for PRE (Fig. 3d). This is likely the consequence of a dominance of evergreen species in
387 the tropics in our data set, but we cannot conclude that the lower amount of data for PRE is
388 also a driver of this pattern. The inconsistencies of patterns and significance in P resorption
389 can be related to high biochemical divergence in leaf P fractions compared to N, leading to
390 varied mobilization paths (Estiarte et al., 2023). The breakdown of proteins is the main way
391 N moves around as 75-80% of N is allocated in proteins, while P mobilization involves many
392 different catabolic pathways that lead to wider variety in P dynamics in leaves during leaf
393 development (Estiarte et al., 2023).

394 We observe no statistical difference between leaf types for NRE (Fig. 3). The higher PRE in
395 needle- than broad-leaves (Fig. 3e) is likely a species effect since almost all needle
396 observations for PRE are plants of the same family, *Pinaceae*. Nevertheless, leaf type is also
397 a strong driver for variance in NRE and PRE (Table 3; Fig. 5). This finding goes together
398 with the view of thicker, longer-lived leaves - such as evergreens and needle-leaves - having
399 lower resorption efficiencies. One possible explanation for this global leaf habit and type
400 pattern is that thicker leaves from evergreens plants, i.e. those with low SLA, have more N
401 allocated to structural leaf compartments, which means it is harder to break down and resorb
402 nutrients back, leading to less resorption. This is different to deciduous plants, in which
403 leaves are characterized by a higher SLA and a larger N investment into metabolic
404 compounds (Onoda et al., 2017). Although SLA is not directly selected in the statistical

405 model, our results implicitly contain the effects of SLA on nutrient resorption through the
406 strong and known relationship between SLA and leaf type and habit (Fig. C4).

407 The leaf economics spectrum (LES) distinguishes "fast" and "slow" economic strategies
408 found globally and existing independent of climate (Wright et al., 2004). A rapid return on
409 investments, or "fast" economic strategy, is typically associated with deciduous plants and
410 achieved through a combination of traits such as shorter leaf longevity, higher nutrient
411 concentrations, and thinner leaves (high SLA), resulting in higher gas exchange rates per unit
412 mass/area (Reich et al., 1992, 1997; Wright et al., 2004). Conversely, a slow return on
413 investments is associated with the opposite set of traits and typically found in evergreen
414 plants (Reich et al., 1992, 1997; Wright et al., 2004). The low SLA of long-lived leaves is
415 associated with low photosynthetic N-use efficiency, but with nutrient investment spread over
416 a longer period. The low photosynthetic N-use efficiency can be attributed to a higher
417 proportion of C and N being allocated to structural rather than metabolic components of the
418 leaf (Reich et al., 2017), which aligns with the theory on leaf carbon optimization proposed
419 by Kikuzawa (1995) and posits that shorter leaf longevity is associated with higher
420 photosynthetic rates or lower costs of leaf construction.

421 Here, we find that plants with a conservative nutrient resorption strategy are located at the
422 non-conservative end of the LES, that is, in the "fast" economic strategy. The discussion that
423 revolves around the LES is determined by a combination of trade-offs between investments
424 in structural and metabolic components, as well as trade-offs over time in the expected
425 returns on those investments (Reich et al., 2017). The non-transferable and possibly
426 transferable nutrients depend on where they are located in the cell and their biochemistry
427 (Estiarte et al., 2023). Metabolic fractions are considered to be fully accessible for resorption
428 while structural fractions have been considered non-degradable (Estiarte et al., 2023). Wang
429 et al. (2023) brings the worldwide pattern of high leaf lifespan (LLS) in plants with low SLA
430 as a natural selection response to maximize carbon gain during leaf development, with
431 variations in SLA in deciduous and evergreen species being determined by microclimate
432 conditions. This pattern scales up from the organ level to a broader perspective that
433 encompasses the trade-off between growth and survival at the plant level (Kikuzawa and
434 Lechowicz, 2011). We find higher NRE in shrubs than trees as observed in previous studies
435 (Yuan and Chen, 2009; Yan et al., 2018; Xu et al., 2021), which is also reflected in the
436 identification of plant growth form as one of the main driving factors for NRE in the

437 multimodel inference analysis (Table 3; Fig. 5a). Compared to trees, shrubs typically have
438 smaller leaves and shorter leaf-lifespans. With that they need to be more resourceful with the
439 nutrients available and prioritize nutrient resorption as a way to optimize nutrient usage for
440 growth.

441 Resorption is an internal plant process that aims to maintain the balance of soil-plant
442 interactions in the acquisition and conservation of nutrients, considering which process is less
443 costly for the plant. The efficiency in nutrient-use by plants is determined mainly by the
444 nutrient residence time in the plant, in which they can access through the leaf longevity
445 maintaining the nutrients or through resorption before leaf abscission (Veneklaas, 2022). Our
446 results support the concept that nutrient resorption is mainly driven by the share of metabolic
447 vs total leaf N and P, which co-varies with SLA (proxy for construction costs).

448 Therefore, higher resorption in deciduous trees may be an important conservation strategy as
449 this process is less energetically costly than new growth. Brant and Chen (2015) discuss the
450 dependence of deciduous trees on nutrient resorption efficiency as their investment in green
451 leaf nutrients is higher to keep fast physiological activity during growing season, or the entire
452 nutrient economy is compromised. With that, we can argue that leaf longevity may be an
453 important strategy for evergreen plants to conserve their lower leaf nutrient content, as the
454 nutrient residence time is higher in evergreens. These plants retain nutrients for as long as
455 possible, because once the nutrients are transferred to the soil through litterfall, they are
456 partially lost from the system.

457

458 **4.2 Effects of climate factors**

459 Our global dataset shows that NRE significantly increases from tropical to polar zones (Fig.
460 2a), while PRE is lowest in temperate zones and significantly increases toward the poles (Fig.
461 2b). This suggests that the resorption of both nutrients is governed to some extent by a
462 comparable dependency on climate, possibly related to slowed soil organic matter
463 decomposition at lower temperatures, which reduces the net rate of mineralization and in
464 turn, limits the availability of nutrients for plant uptake from the soil (Sharma and Kumar,
465 2023). MAT emerges as one of the main drivers for PRE but not for NRE (Table 3). This
466 result may be the outcome of the overall distribution of deciduous and evergreen species
467 across climate zones, suggesting that global variations in N and P resorption along climatic
468 gradients may arise primarily from global patterns in deciduous vs. evergreen and

469 needle-leaved vs. broadleaved plants. This statement is important in the context of projecting
470 nutrient cycling under altered climate and indicates limited responses in resorption to
471 temporal changes in climate at decadal time scales – before the global distribution of leaf
472 habit and type changes as a result of shifts in species composition.

473 MAP emerges as an important driver for NRE (Table 3; Fig. 5). One explanation is that low
474 MAP leads to low soil moisture, constraining nutrient mobility and increasing the carbon cost
475 for plants to take up nutrients (Gill and Finzi, 2016). Therefore, together with limited N
476 resorption mobility in leaf tissues discussed above (Estiarte and Peñuelas, 2015), soil
477 moisture constrains N mobilization during the mineralization process (Thamdrup, 2012). Liu
478 et al. (2017) analyzed the relation between soil N mineralization and temperature sensitivity
479 on a global scale, and showed largest N mineralization rates at tropical latitudes and a general
480 poleward decrease. We can observe a similar pattern of NRE with latitude (Fig. C3). Deng et
481 al. (2018) observed a negative relationship between NRE and mineralisation rate, which
482 suggests a reciprocal causal relationship where systems emerge exhibiting either
483 simultaneously low mineralization and high resorption rates. The strong link we find here
484 between NRE and leaf habit and leaf type - traits that are immutable within a given species -
485 indicates that the variations we observe in resorption might be a possible reflection of species
486 composition with direct consequence for N cycling. It suggests that a positive feedback
487 mechanism exists that leads ecosystems to be characterized by high resorption and a slower
488 soil cycling, or vice versa (Phillips et al., 2013). For example, species adapted to low soil N
489 are favored in N-limited environments, but they also produce low-N litter that decreases
490 mineralisation and further favors their competitiveness (Chapin et al., 2011).

491 In addition, we find a negative correlation between resorption and GSL (Figs. C1). Plant
492 strategies in regions with short growing seasons (e.g. high latitudes or seasonally dry
493 subtropical regions) are focused on nutrient conservation to maximize growth during the
494 favorable period, despite nutrient availability. In very cold and seasonal environments, as
495 seen in grassy tundra vegetation, soil nutrients are often not available concurrently with plant
496 demand (Lacroix et al., 2022), implying that it may be more advantageous for plants to retain
497 their nutrients. While we did not include GSL in the multimodel inference analysis due to its
498 high collinearity with MAT, this aspect is partially reflected in leaf habit.

499 When we separate the global patterns for different climate zones and PFTs, our results show
500 that the major climatic pattern is consistent across the growth forms and leaf types and leaf

501 habit (Fig. 4), in which NRE and PRE increases towards higher latitudes and PRE shows a
502 minimum at mid-latitudes. Our findings support that maximum NRE and PRE may be firstly
503 constrained by leaf properties, with secondary effects from climate and soil texture (discussed
504 below). Estiarte et al. (2023) suggest that a plant's leaf biochemistry (biochemical and
505 subcellular fractions of N and P) is the primary factor in limiting nutrient resorption, followed
506 by secondary regulation related to environmental conditions in space and time. They present
507 that resorption efficiency declines when soil nutrient availability rises, as plant uptake
508 becomes less costly in more fertile soil. However, the expenses linked to aging leaves remain
509 constant (Estiarte et al., 2023).

510

511 **4.3 Effect of soil nutrient availability**

512 N and P deposition and clay content emerge as important predictors for both PRE and NRE
513 (Table 3; Fig. 5). This likely reflects the influence of soil N and P availability for NRE and
514 PRE. Clay content is an important factor determining the nutrient retention capacity and
515 cation exchange capacity in soils (Chapin et al., 2011). Chronic N deposition has increased
516 soil N availability (Galloway et al., 2004) and leaf nutrient content (Chapin et al., 2011) over
517 the 20th century, and likely affected plant internal recycling and resorption as indicated by our
518 spatial results. In a fertilization experiment, higher P input had a negative effect on both NRE
519 and PRE (Yuan and Chen, 2015), suggesting that increased P deposition may reduce the plant
520 internal recycling and thus resorption. The cycling and accessibility of soil P are influenced
521 by N deposition (Marklein and Houlton, 2012) through various mechanisms, including
522 changes in plant P use strategies (Dalling et al., 2016; Wu et al., 2020a). Higher N deposition
523 tends to reduce total soil P content (Sardans et al., 2016) so plants would need to increase
524 PRE to compensate for the high soil N:P stoichiometry and P limitation. Jonard et al. (2015)
525 suggested that forest ecosystems are becoming less efficient at recycling P due to excessive N
526 input and climatic stress. This observation likely contributes to our finding that N and P
527 deposition emerge as a stronger driver in a negative correlation with PRE (Fig. 5; Table 3;
528 Figs. C1). The lack of effect by total soil P on NRE and PRE may result from the fact that
529 this variable does not represent the actual fraction of P available for plant uptake.
530 Nevertheless, N deposition has a strong positive effect on NRE (Fig. 5; Table 3) – contrary to
531 expectations (Aerts and Chapin, 1999; Yuan and Chen, 2015; Fisher et al., 2010). This
532 indicates that the influence of N deposition might be via effects on SLA, whereby increasing

533 N deposition increases the fraction of non-structurally bound N and therefore increases the
534 fraction of N that can be resorbed. This effect, corrected for covariant factors such as leaf
535 type and growth form, overlaps the negative effect of soil clay content on NRE and PRE
536 which suggests that resorption decreases with nutrient availability in clay-rich soils. Our
537 results raise an important point on the correlation of leaf nutrient resorption and nutrient
538 limitation, showing that the relationships are complex and driven by multiple interacting and
539 seemingly opposing factors.

540 Another soil factor we find to be important for nutrient resorption is the clay content (Table
541 3). Clay minerals are formed during soil weathering and have high surface area that
542 influences the soil's water retention capacity, and a negative charge that enables nutrients
543 retention and exchange with plant roots (Chapin et al., 2011). High-latitude soils that are
544 younger and experience slow rates of chemical weathering usually have low clay content and
545 therefore, less potential for mineral nutrient storage, which may affect their availability for
546 plant uptake (Chapin et al., 2011). As a result, plants in these environments need to invest
547 more in resorption. Thus, together with MAP and MAT, soil clay content is also closely
548 related to soil nutrient supply on a global scale, which is reflected in its role as driving
549 resorption (Table 3; Fig. 5), as well as in the negative correlation between clay content and
550 nutrient resorption (Figs. C1). The important effect of leaf properties on nutrient resorption,
551 along with climate, soil texture, and soil fertility (as previously suggested by Aerts and
552 Chapin, 1999; Yuan and Chen, 2015; Xu et al., 2021), may indicate that biological and
553 environmental factors are interconnected, as it is also influenced by multiple elements such as
554 litter quality, precipitation, parent materials, and soil texture. For example, P availability is
555 geologically and pedologically limited in warm environments, which means mainly
556 determined by soil parent materials (Augusto et al., 2017), and therefore, soil texture
557 becomes an important factor for P limitation in tropical regions. Also, the role of P deposition
558 in relation to plant demand is high for tropical forests (Van Langenhove et al., 2020) but low
559 worldwide (Cleveland et al., 2013). PRE in the tropics do not differ statistically from other
560 climate zones although we observe an increase of PRE from mid to low latitudes (Figs. B1b
561 and C3), which may indicate data limitation for PRE. The combination of plant properties
562 with an underlying soil and climate control as driving factors for resorption variation is also
563 supported by Drenovsky et al. (2010; 2019), who suggested a combination of soil properties,
564 climatic factors, and plant morphology to explain changes in nutrient resorption.

565

566 **4.4 Data uncertainties and implications**

567 Our study contributes to the existing research on nutrient resorption by using a
568 comprehensive approach to derive resorption values from the TRY database. However, we
569 encounter limitations in this derivation due to a lack or limited quality of data. The absence of
570 co-located nutrient measurements in leaf and litter led to a shortage of suitable data pairs,
571 mainly for PRE, in which the robustness of the model selection raised concerns about its
572 reliability. In addition, it is not possible to assess the entire temporal aspect of data collection,
573 which increases intraspecific variability. For NRE, 645 of a total of 954 observations are from
574 the same growing season, as we have collection information for green leaves and litter
575 samples whether they were picked from the plant, recently fallen or from litterfall traps
576 cleared every week. Consequently, for approximately 30% of the data, we cannot confirm
577 that the leaf and litter measurements are from the same growing season and legitimately from
578 the same individual. This is indeed one of the greatest limitations in assessing reliable
579 nutrient resorption values. Nevertheless, it remains the accepted - and only - method for
580 evaluating resorption on a broad scale.

581 While our approach of accounting for the MLCF improves estimates of resorption (Appendix
582 A), we could not estimate the MLCF for all data pairs, as well as fill all gaps using average
583 functional type characteristics due to the lack of trait attributes in the TRY database. These
584 two factors reduce the number of data points available for statistical analysis using
585 multi-model inference. Furthermore, although we recognize the importance of leaf lifespan
586 (LLS), it is not possible to analyze the relationship between resorption and LLS due to the
587 few measurements of this functional trait. Nevertheless, applying the available statistical
588 methods to analyze the drivers behind NRE and PRE, we find consistent patterns for the key
589 gradients of climate, soil and PFTs, that are informative for other studies despite remaining
590 unexplained variance. In addition, we find that even within species of the same family, the
591 distribution of NRE values is nearly as wide as the distribution for PFTs. This coordination in
592 the observed spread likely reflects a substantial contribution from environmental variability,
593 which would be interesting for further analysis if more data is available. In order to improve
594 the depth of resorption investigation, we encourage researchers in field work to perform
595 concurrent measurements of litter nutrient content as well as leaf and litter dry mass.

596 The statistical analysis of dredge multi-model inference depends on the specific factors used
597 in the analysis. We removed highly collinear variables and tested the impact of different
598 combinations of factors. Although changing the factors affects the exact number of data
599 points used in each multi-model inference, the overall identification of important and less
600 important factors for NRE and PRE remains robust, especially for PFTs. However, ensuring
601 that our analysis is as global as possible, the statistical dredge model analysis can
602 consequently be influenced by temperate regions bias, which is an inherent limitation we
603 cannot fully mitigate but one that is present in any global meta-analysis of this kind.

604 By quantifying these trends that we have found, we can delve deeper into ecosystem models
605 by improving model parametrization and developing a dynamic nutrient resorption concept.
606 Studies that utilize data to infer nutrient cycling frequently simplify resorption making
607 general assumptions (Finzi et al., 2007; Cleveland et al., 2013), or simply representing this
608 process as a fixed value of 50% (Vergutz et al., 2012; Zaehle et al. 2014), which may cause
609 inaccuracies in their findings on nutrient cycling. The flow of recycling nutrients in land
610 surface models is a factor that determines how strong the soil nutrient availability controls
611 plant production. N resorption and N uptake in the FUN model (Fisher et al., 2010), for
612 example, is defined by the relative acquisition cost of the two sources. They discuss that the
613 cost of resorption assumes a constant based on global observations, but it may require a
614 clearer connection to leaf physiology. Here, we provide a start for a statistical model that can
615 connect resorption and plant properties and restrict how much plants could actually resorb
616 nutrients, as well as the dataset to test the predictions of a physiological model. In addition,
617 environmental drivers that have been shown to influence the overall patterns, such as soil
618 texture and climate, could be considered to influence the resorption efficiency after primary
619 leaf physiology limitation. Such information is essential when estimating how it can constrain
620 carbon assimilation in face of global changes (Galloway et al., 2008), and therefore, essential
621 to predict future plant growth and the capacity of the forest to act as a carbon sink (Thornton
622 et al., 2007; Arora et al., 2022).

623

624 **5. Conclusions**

625 Our analysis of the global plant trait database indicates that variations of NRE and PRE are
626 driven by the combination of plant properties with an additional soil and climate control.
627 Systematic variations of NRE across leaf habit and type indicate that these traits are linked to

628 plant nutrient use and conservation strategies and that leaf structure plays an important role in
629 determining the proportion of nutrients that can be resorbed. Different metrics of soil fertility
630 and soil-related variables influence NRE and PRE together with climatic variables and leaf
631 structure and habit. Clay content, N and P deposition have a strong influence with a negative
632 relationship - possibly an expression of its role in nutrient retention - as well as MAP. These
633 trends provide a target to benchmark the simulation of nutrient recycling in global
634 nutrient-enabled models. A focus on considering the links between leaf structure and nutrient
635 resorption efficiency should enable a more realistic consideration of ecological and
636 environmental controls on nutrient cycling and limitation than the current state-of-the-art.
637 The importance of intrinsic plant properties raises important questions about the flexibility of
638 leaf resorption under future changes in climate, CO₂ concentrations and atmospheric
639 deposition.

640

641 **Acknowledgments**

642 This work was supported by the European Research Council (ERC) under the European
643 Union's Horizon 2020 research and innovation programme (QUINCY; grant no. 647204).
644 BDS was funded by the Swiss National Science Foundation grant PCEFP2_181115. We
645 extend our thanks to our external reviewer Katrin Fleisher, for her helpful comments on the
646 manuscript.

647 **Author contributions**

648 GS, SC and SZ designed the study. GS performed the analysis. All authors contributed to
649 interpreting the results. GS drafted the manuscripts; all authors contributed to writing and
650 editing the manuscript.

651 **Data Availability Statement**

652 All data used in this study is publicly available through the TRY database
653 <https://www.try-db.org/>.

654 **Conflict of Interests**

655 SZ is a member of the editorial board of Biogeosciences.

656 **References**

657 Aerts, R.: Nutrient Resorption from Senescing Leaves of Perennials: Are there General
658 Patterns?, *Journal of Ecology*, 84, 1996.

659

660 Aerts, R. and Chapin, F. S.: The Mineral Nutrition of Wild Plants Revisited: A Re-evaluation
661 of Processes and Patterns, in: *Advances in Ecological Research*, vol. 30, edited by: Fitter, A.
662 H. and Raffaelli, D. G., Academic Press, 1–67, 1999.

663

664 Arora, V. K., Seiler, C., Wang, L., and Kou-Giesbrecht, S.: Towards an ensemble-based
665 evaluation of land surface models in light of uncertain forcings and observations, *EGUsphere*,
666 <https://doi.org/10.5194/egusphere-2022-641>, 2022.

667

668 Augusto, L., Achat, D. L., Jonard, M., Vidal, D., and Ringeval, B.: Soil parent material-A
669 major driver of plant nutrient limitations in terrestrial ecosystems, *Glob. Chang. Biol.*, 23,
670 3808–3824, 2017.

671

672 Bartoń, K.: MuMIn: multi-model inference, R package version 1.47.5, 2023.

673

674 Bazzaz, F. A.: The Response of Natural Ecosystems to the Rising Global CO₂ Levels, *Annu.*
675 *Rev. Ecol. Syst.*, 21, 167–196, 1990.

676

677 Berg, B. and McClaugherty, C. A.: *Plant Litter. Decomposition, Humus Formation, Carbon*
678 *Sequestration*, Springer Verlag, 2014.

679

680 Brahney, J., Mahowald, N., Ward, D. S., Ballantyne, A. P., and Neff, J. C.: Is atmospheric
681 phosphorus pollution altering global alpine Lake stoichiometry?, *Global Biogeochem.*
682 *Cycles*, 29, 1369–1383, 2015.

683

684 Brant, A. N. and Chen, H. Y. H.: Patterns and Mechanisms of Nutrient Resorption in Plants,
685 *CRC Crit. Rev. Plant Sci.*, 34, 471–486, 2015.

686

687 Bryant, C., Wheeler, N. R., Rubel, F., French, R. H.: *kgc: Koeppen-Geiger Climatic Zones*, R
688 package version 1.0.0.2, 2017.

689

690 Burnham, K. P. and Anderson, D. R.: *Model Selection and Inference*, Springer New York, 20
691 pp., n.d.

692

693 Chapin, F. S.: The Mineral Nutrition of Wild Plants, *Annu. Rev. Ecol. Syst.*, 11, 233–260,
694 1980.

695

696 Chapin, F. S., Matson, P. A., and Vitousek, P. M.: Principles of Terrestrial Ecosystem
697 Ecology, Springer, New York, NY, 2011.

698

699 Chen, H., Reed, S. C., Lü, X., Xiao, K., Wang, K., and Li, D.: Coexistence of multiple leaf
700 nutrient resorption strategies in a single ecosystem, *Sci. Total Environ.*, 772, 144951, 2021.

701

702 Chien, C.-T., Mackey, K. R. M., Dutkiewicz, S., Mahowald, N. M., Prospero, J. M., and
703 Paytan, A.: Effects of African dust deposition on phytoplankton in the western tropical
704 Atlantic Ocean off Barbados, *Global Biogeochem. Cycles*, 30, 716–734, 2016.

705

706 Cleveland, C. C., Houlton, B. Z., Smith, W. K., Marklein, A. R., Reed, S. C., Parton, W., Del
707 Grosso, S. J., and Running, S. W.: Patterns of new versus recycled primary production in the
708 terrestrial biosphere, *Proc. Natl. Acad. Sci. U. S. A.*, 110, 12733–12737, 2013.

709

710 Dalling, J. W., Heineman, K., Lopez, O. R., Wright, S. J., and Turner, B. L.: Nutrient
711 Availability in Tropical Rain Forests: The Paradigm of Phosphorus Limitation, in: *Tropical
712 Tree Physiology: Adaptations and Responses in a Changing Environment*, edited by:
713 Goldstein, G. and Santiago, L. S., Springer International Publishing, Cham, 261–273, 2016.

714

715 Deng, M., Liu, L., Jiang, L., Liu, W., Wang, X., Li, S., Yang, S., and Wang, B.: Ecosystem
716 scale trade-off in nitrogen acquisition pathways, *Nat Ecol Evol*, 2, 1724–1734, 2018.

717

718 Drenovsky, R. E., James, J. J., and Richards, J. H.: Variation in nutrient resorption by desert
719 shrubs, *J. Arid Environ.*, 74, 1564–1568, 2010.

720

721 Drenovsky, R. E., Pietrasiak, N., and Short, T. H.: Global temporal patterns in plant nutrient
722 resorption plasticity, *Glob. Ecol. Biogeogr.*, 28, 728–743, 2019.

723

724 Du, E., Terrer, C., Pellegrini, A. F. A., Ahlström, A., van Lissa, C. J., Zhao, X., Xia, N., Wu,
725 X., and Jackson, R. B.: Global patterns of terrestrial nitrogen and phosphorus limitation,
726 <https://doi.org/10.1038/s41561-019-0530-4>, 2020.

727

728 Elser, J. J., Bracken, M. E. S., Cleland, E. E., Gruner, D. S., Harpole, W. S., Hillebrand, H.,
729 Ngai, J. T., Seabloom, E. W., Shurin, J. B., and Smith, J. E.: Global analysis of nitrogen and
730 phosphorus limitation of primary producers in freshwater, marine and terrestrial ecosystems,
731 *Ecol. Lett.*, 10, 1135–1142, 2007.

732

733 Estiarte, M. and Peñuelas, J.: Alteration of the phenology of leaf senescence and fall in winter
734 deciduous species by climate change: effects on nutrient proficiency, *Glob. Chang. Biol.*, 21,
735 1005–1017, 2015.

736

737 Estiarte, M., Campioli, M., Mayol, M., and Peñuelas, J.: Variability and limits of nitrogen and
738 phosphorus resorption during foliar senescence, *Plant Comm*, 4,
739 <https://doi.org/10.1016/j.xplc.2022.100503>, 2023.

740

741 Fay, P. A., Prober, S. M., Harpole, W. S., Knops, J. M. H., Bakker, J. D., Borer, E. T., Lind, E.
742 M., MacDougall, A. S., Seabloom, E. W., Wragg, P. D., Adler, P. B., Blumenthal, D. M.,
743 Buckley, Y. M., Chu, C., Cleland, E. E., Collins, S. L., Davies, K. F., Du, G., Feng, X., Firn,
744 J., Gruner, D. S., Hagenah, N., Hautier, Y., Heckman, R. W., Jin, V. L., Kirkman, K. P., Klein,
745 J., Ladwig, L. M., Li, Q., McCulley, R. L., Melbourne, B. A., Mitchell, C. E., Moore, J. L.,
746 Morgan, J. W., Risch, A. C., Schütz, M., Stevens, C. J., Wedin, D. A., and Yang, L. H.:
747 Grassland productivity limited by multiple nutrients, *Nat Plants*, 1, 15080, 2015.

748

749 Fick, S. E. and Hijmans, R. J.: WorldClim 2: new 1-km spatial resolution climate surfaces for
750 global land areas, *Int. J. Climatol.*, 37, 4302–4315, 2017.

751

752 Finzi, A. C., Norby, R. J., Calfapietra, C., Gallet-Budynek, A., Gielen, B., Holmes, W. E.,
753 Hoosbeek, M. R., Iversen, C. M., Jackson, R. B., Kubiske, M. E., Ledford, J., Liberloo, M.,
754 Oren, R., Polle, A., Pritchard, S., Zak, D. R., Schlesinger, W. H., and Ceulemans, R.:
755 Increases in nitrogen uptake rather than nitrogen-use efficiency support higher rates of
756 temperate forest productivity under elevated CO₂, *Proc. Natl. Acad. Sci. U. S. A.*, 104,
757 14014–14019, 2007.

758

759 Fisher, J. B., Sitch, S., Malhi, Y., Fisher, R. A., Huntingford, C., and Tan, S.-Y.: Carbon cost
760 of plant nitrogen acquisition: A mechanistic, globally applicable model of plant nitrogen
761 uptake, retranslocation, and fixation, *Global Biogeochem. Cycles*, 24,
762 <https://doi.org/10.1029/2009gb003621>, 2010.

763

764 Galloway, J. N., Dentener, F. J., Capone, D. G., Boyer, E. W., Howarth, R. W., Seitzinger, S.
765 P., Asner, G. P., Cleveland, C. C., Green, P. A., Holland, E. A., Karl, D. M., Michaels, A. F.,
766 Porter, J. H., Townsend, A. R., and Vöosmarty, C. J.: Nitrogen Cycles: Past, Present, and
767 Future, *Biogeochemistry*, 70, 153–226, 2004.

768

769 Galloway, J. N., Townsend, A. R., Erisman, J. W., Bekunda, M., Cai, Z., Freney, J. R.,
770 Martinelli, L. A., Seitzinger, S. P., and Sutton, M. A.: Transformation of the nitrogen cycle:
771 recent trends, questions, and potential solutions, *Science*, 320, 889–892, 2008.

772

773 Gill, A. L. and Finzi, A. C.: Belowground carbon flux links biogeochemical cycles and
774 resource-use efficiency at the global scale, *Ecol. Lett.*, 19, 1419–1428, 2016.

775

776 Güsewell, S.: N : P ratios in terrestrial plants: variation and functional significance, *New
777 Phytol.*, 164, 243–266, 2004.

778

779 Han, W., Tang, L., Chen, Y., and Fang, J.: Relationship between the relative limitation and
780 resorption efficiency of nitrogen vs phosphorus in woody plants, *PLoS One*, 8, e83366, 2013.

781

782 Hedin, L. O., Brookshire, E. N. J., Menge, D. N. L., and Barron, A. R.: The Nitrogen Paradox
783 in Tropical Forest Ecosystems, *Annu. Rev. Ecol. Evol. Syst.*, 40, 613–635, 2009.

784

785 Hegglin, M., Kinnison, D., and Lamarque, J.-F.: CCM1 nitrogen surface fluxes in support of
786 CMIP6 - version 2.0, <https://doi.org/10.22033/ESGF/input4MIPs.1125>, 2016.

787

788 James, G., Witten, D., Hastie, T., and Tibshirani, R.: *An Introduction to Statistical Learning:
789 with Applications in R*, Springer, New York, ISBN 978-1-4614-7138-7, 2013.

790

791 Jonard, M., Fürst, A., Verstraeten, A., Thimonier, A., Timmermann, V., Potočić, N., Waldner,
792 P., Benham, S., Hansen, K., Merilä, P., Ponette, Q., de la Cruz, A. C., Roskams, P., Nicolas,
793 M., Croisé, L., Ingerslev, M., Matteucci, G., Decinti, B., Bascietto, M., and Rautio, P.: Tree
794 mineral nutrition is deteriorating in Europe, *Glob. Chang. Biol.*, 21, 418–430, 2015.

795

796 Jung, M., Reichstein, M., Margolis, H. A., Cescatti, A., Richardson, A. D., Arain, M. A.,
797 Arneth, A., Bernhofer, C., Bonal, D., Chen, J., Gianelle, D., Gobron, N., Kiely, G., Kutsch,
798 W., Lasslop, G., Law, B. E., Lindroth, A., Merbold, L., Montagnani, L., Moors, E. J., Papale,
799 D., Sottocornola, M., Vaccari, F., and Williams, C.: Global patterns of land-atmosphere fluxes
800 of carbon dioxide, latent heat, and sensible heat derived from eddy covariance, satellite, and
801 meteorological observations, *J. Geophys. Res.*, 116, <https://doi.org/10.1029/2010jg001566>,
802 2011.

803

804 Kattge, J., Díaz, S., Lavorel, S., Prentice, I. C., Leadley, P., Bönlisch, G., Garnier, E., Westoby,
805 M., Reich, P. B., Wright, I. J., Cornelissen, J. H. C., Violle, C., Harrison, S. P., Van
806 BODEGOM, P. M., Reichstein, M., Enquist, B. J., Soudzilovskaia, N. A., Ackerly, D. D.,
807 Anand, M., Atkin, O., Bahn, M., Baker, T. R., Baldocchi, D., Bekker, R., Blanco, C. C.,
808 Blonder, B., Bond, W. J., Bradstock, R., Bunker, D. E., Casanoves, F., Cavender-Bares, J.,
809 Chambers, J. Q., Chapin, F. S., Iii, Chave, J., Coomes, D., Cornwell, W. K., Craine, J. M.,
810 Dobrin, B. H., Duarte, L., Durka, W., Elser, J., Esser, G., Estiarte, M., Fagan, W. F., Fang, J.,
811 Fernández-Méndez, F., Fidelis, A., Finegan, B., Flores, O., Ford, H., Frank, D., Freschet, G.
812 T., Fyllas, N. M., Gallagher, R. V., Green, W. A., Gutierrez, A. G., Hickler, T., Higgins, S. I.,
813 Hodgson, J. G., Jalili, A., Jansen, S., Joly, C. A., Kerkhoff, A. J., Kirkup, D., Kitajima, K.,
814 Kleyer, M., Klotz, S., Knops, J. M. H., Kramer, K., Kühn, I., Kurokawa, H., Laughlin, D.,
815 Lee, T. D., Leishman, M., Lens, F., Lenz, T., Lewis, S. L., Lloyd, J., Llusià, J., Louault, F.,
816 Ma, S., Mahecha, M. D., Manning, P., Massad, T., Medlyn, B. E., Messier, J., Moles, A. T.,
817 Müller, S. C., Nadrowski, K., Naeem, S., Niinemets, Ü., Nöllert, S., Nüske, A., Ogaya, R.,

818 Oleksyn, J., Onipchenko, V. G., Onoda, Y., Ordoñez, J., Overbeck, G., et al.: TRY - a global
819 database of plant traits, *Glob. Chang. Biol.*, 17, 2905–2935, 2011.

820

821 Kattge, J., Bönisch, G., Díaz, S., Lavorel, S., Prentice, I. C., Leadley, P., Tautenhahn, S.,
822 Werner, G. D. A., Aakala, T., Abedi, M., Acosta, A. T. R., Adamidis, G. C., Adamson, K.,
823 Aiba, M., Albert, C. H., Alcántara, J. M., Alcázar, C. C., Aleixo, I., Ali, H., Amiaud, B.,
824 Ammer, C., Amoroso, M. M., Anand, M., Anderson, C., Anten, N., Antos, J., Apgaua, D. M.
825 G., Ashman, T.-L., Asmara, D. H., Asner, G. P., Aspinwall, M., Atkin, O., Aubin, I.,
826 Bastrup-Spohr, L., Bahalkeh, K., Bahn, M., Baker, T., Baker, W. J., Bakker, J. P., Baldocchi,
827 D., Baltzer, J., Banerjee, A., Baranger, A., Barlow, J., Barneche, D. R., Baruch, Z.,
828 Bastianelli, D., Battles, J., Bauerle, W., Bauters, M., Bazzato, E., Beckmann, M., Beeckman,
829 H., Beierkuhnlein, C., Bekker, R., Belfry, G., Belluau, M., Beloiu, M., Benavides, R.,
830 Benomar, L., Berdugo-Lattke, M. L., Berenguer, E., Bergamin, R., Bergmann, J., Bergmann
831 Carlucci, M., Berner, L., Bernhardt-Römermann, M., Bigler, C., Bjorkman, A. D., Blackman,
832 C., Blanco, C., Blonder, B., Blumenthal, D., Bocanegra-González, K. T., Boeckx, P.,
833 Bohlman, S., Böhning-Gaese, K., Boisvert-Marsh, L., Bond, W., Bond-Lamberty, B., Boom,
834 A., Boonman, C. C. F., Bordin, K., Boughton, E. H., Boukili, V., Bowman, D. M. J. S.,
835 Bravo, S., Brendel, M. R., Broadley, M. R., Brown, K. A., Bruelheide, H., Brumnich, F.,
836 Bruun, H. H., Bruy, D., Buchanan, S. W., Bucher, S. F., Buchmann, N., Buitenwerf, R.,
837 Bunker, D. E., et al.: TRY plant trait database - enhanced coverage and open access, *Glob.*
838 *Chang. Biol.*, 26, 119–188, 2020.

839

840 Kikuzawa, K.: Leaf phenology as an optimal strategy for carbon gain in plants, *Can. J. Bot.*,
841 <https://doi.org/10.1139/b95-019>, 1995.

842

843 Kikuzawa, K. and Lechowicz, M. J.: *Ecology of leaf longevity*, 2011th ed., Springer, Tokyo,
844 Japan, 147 pp., 2011.

845

846 Killingbeck, K. T.: Nutrients in senesced leaves: Keys to the search for potential resorption
847 and resorption proficiency, *Ecology*, 77, 1716–1727, 1996.

848

849 Kobe, R. K., Lepczyk, C. A., and Iyer, M.: Resorption efficiency decreases with increasing
850 green leaf nutrients in a global data set, *Ecology*, 86, 2780–2792, 2005.

851

852 Lacroix, F., Zaehle, S., Caldararu, S., Schaller, J., Stimmler, P., Holl, D., Kutzbach, L., and
853 Goeckede, M.: Decoupling of permafrost thaw and vegetation growth could mean both
854 ongoing nutrient limitation and an emergent source of N₂O in high latitudes, *Earth and Space*
855 *Science Open Archive*, <https://doi.org/10.1002/essoar.10510605.1>, 2022.

856

857 Lam, O. H. Y., Tautenhahn, S., Walther, G., Boenisch, G., Baddam, P., and Kattge, J.: The
858 “rtry” R package for preprocessing plant trait data,
859 <https://doi.org/10.5194/egusphere-egu22-13251>, 2022.

860

861 Lawrence, D. M., Fisher, R. A., Koven, C. D., Oleson, K. W., Swenson, S. C., Bonan, G.,
862 Collier, N., Ghimire, B., van Kampenhout, L., Kennedy, D., Kluzek, E., Lawrence, P. J., Li,
863 F., Li, H., Lombardozzi, D., Riley, W. J., Sacks, W. J., Shi, M., Vertenstein, M., Wieder, W.
864 R., Xu, C., Ali, A. A., Badger, A. M., Bisht, G., van den Broeke, M., Brunke, M. A., Burns,
865 S. P., Buzan, J., Clark, M., Craig, A., Dahlin, K., Drewniak, B., Fisher, J. B., Flanner, M.,
866 Fox, A. M., Gentine, P., Hoffman, F., Keppel-Aleks, G., Knox, R., Kumar, S., Lenaerts, J.,
867 Leung, L. R., Lipscomb, W. H., Lu, Y., Pandey, A., Pelletier, J. D., Perket, J., Randerson, J.
868 T., Ricciuto, D. M., Sanderson, B. M., Slater, A., Subin, Z. M., Tang, J., Thomas, R. Q., Val
869 Martin, M., and Zeng, X.: The community land model version 5: Description of new features,
870 benchmarking, and impact of forcing uncertainty, *J. Adv. Model. Earth Syst.*, 11, 4245–4287,
871 2019.

872

873 LeBauer, D. S. and Treseder, K. K.: Nitrogen limitation of net primary productivity in
874 terrestrial ecosystems is globally distributed, *Ecology*, 89, 371–379, 2008.

875

876 Liu, Y., Wang, C., He, N., Wen, X., Gao, Y., Li, S., Niu, S., Butterbach-Bahl, K., Luo, Y., and
877 Yu, G.: A global synthesis of the rate and temperature sensitivity of soil nitrogen
878 mineralization: latitudinal patterns and mechanisms, *Glob. Chang. Biol.*, 23, 455–464, 2017.

879

880 Luo, Y., Su, B., Currie, W. S., Dukes, J. S., Finzi, A., Hartwig, U., Hungate, B., McMurtrie,
881 R. E., Oren, R., Parton, W. J., Pataki, D. E., Shaw, R. M., Zak, D. R., and Field, C. B.:
882 Progressive Nitrogen Limitation of Ecosystem Responses to Rising Atmospheric Carbon
883 Dioxide, *Bioscience*, 54, 731–739, 2004.

884

885 Marklein, A. R. and Houlton, B. Z.: Nitrogen inputs accelerate phosphorus cycling rates
886 across a wide variety of terrestrial ecosystems, *New Phytol.*, 193, 696–704, 2012.

887

888 Onoda, Y., Wright, I. J., Evans, J. R., Hikosaka, K., Kitajima, K., Niinemets, Ü., Poorter, H.,
889 Tosens, T., and Westoby, M.: Physiological and structural tradeoffs underlying the leaf
890 economics spectrum, *New Phytol.*, 214, 1447–1463, 2017.

891

892 Patil, I.: Visualizations with statistical details: The “ggstatsplot” approach, *J. Open Source
893 Softw.*, 6, 3167, 2021.

894

895 Phillips, R. P., Brzostek, E., and Midgley, M. G.: The mycorrhizal-associated nutrient
896 economy: a new framework for predicting carbon-nutrient couplings in temperate forests,
897 *New Phytol.*, 199, 41–51, 2013.

898

899 Reed, S. C., Townsend, A. R., Davidson, E. A., and Cleveland, C. C.: Stoichiometric patterns
900 in foliar nutrient resorption across multiple scales, *New Phytol.*, 196, 173–180, 2012.

901

902 Reich, P. B. and Flores-Moreno, H.: Peeking beneath the hood of the leaf economics
903 spectrum, *New Phytol.*, 214, 1395–1397, 2017.

904

905 Reich, P. B., Walters, M. B., and Ellsworth, D. S.: Leaf Life-Span in Relation to Leaf, Plant,
906 and Stand Characteristics among Diverse Ecosystems, *Ecol. Monogr.*, 62, 365–392, 1992.

907

908 Reich, P. B., Walters, M. B., and Ellsworth, D. S.: From tropics to tundra: global convergence
909 in plant functioning, *Proc. Natl. Acad. Sci. U. S. A.*, 94, 13730–13734, 1997.

910

911 Sardans, J., Alonso, R., Janssens, I. A., Carnicer, J., Vereseglou, S., Rillig, M. C.,
912 Fernández-Martínez, M., Sanders, T. G. M., and Peñuelas, J.: Foliar and soil concentrations
913 and stoichiometry of nitrogen and phosphorous across European *Pinus sylvestris* forests:
914 relationships with climate, N deposition and tree growth, *Funct. Ecol.*, 30, 676–689, 2016.

915

916 Sharma, P. K. and Kumar, S.: Soil Temperature and Plant Growth, in: *Soil Physical
917 Environment and Plant Growth: Evaluation and Management*, edited by: Sharma, P. K. and
918 Kumar, S., Springer International Publishing, Cham, 175–204, 2023.

919

920 Sun, X., Li, D., Lü, X., Fang, Y., Ma, Z., Wang, Z., Chu, C., Li, M., and Chen, H.:
921 Widespread controls of leaf nutrient resorption by nutrient limitation and stoichiometry,
922 *Funct. Ecol.*, 37, 1653–1662, 2023.

923

924 Tang, L., Han, W., Chen, Y., and Fang, J.: Resorption proficiency and efficiency of leaf
925 nutrients in woody plants in eastern China, *J Plant Ecol*, 6, 408–417, 2013.

926

927 Terrer, C., Vicca, S., Hungate, B. A., Phillips, R. P., and Prentice, I. C.: Mycorrhizal
928 association as a primary control of the CO₂ fertilization effect, *Science*, 353, 72–74, 2016.

929

930 Thamdrup, B.: New Pathways and Processes in the Global Nitrogen Cycle, *Annu. Rev. Ecol.
931 Evol. Syst.*, 43, 407–428, 2012.

932

933 Thornton, P. E., Lamarque, J.-F., Rosenbloom, N. A., and Mahowald, N. M.: Influence of
934 carbon-nitrogen cycle coupling on land model response to CO₂ fertilization and climate
935 variability, *Global Biogeochem. Cycles*, 21, <https://doi.org/10.1029/2006gb002868>, 2007.

936

937 Van Heerwaarden, L. M., Toet, S., and Aerts, R.: Current measures of nutrient resorption
938 efficiency lead to a substantial underestimation of real resorption efficiency: facts and
939 solutions, *Oikos*, 101, 664–669, 2003.

940

941 Van Langenhove, L., Verryckt, L. T., Bréchet, L., Courtois, E. A., Stahl, C., Hofhansl, F.,
942 Bauters, M., Sardans, J., Boeckx, P., Fransen, E., Peñuelas, J., and Janssens, I. A.:
943 Atmospheric deposition of elements and its relevance for nutrient budgets of tropical forests,
944 *Biogeochemistry*, 149, 175–193, 2020.

945

946 Veneklaas, E. J.: Phosphorus resorption and tissue longevity of roots and leaves – importance
947 for phosphorus use efficiency and ecosystem phosphorus cycles, *Plant Soil*, 476, 627–637,
948 2022.

949

950 Vergutz, L., Manzoni, S., Porporato, A., Novais, R. F., and Jackson, R. B.: Global resorption
951 efficiencies and concentrations of carbon and nutrients in leaves of terrestrial plants, *Ecol.*
952 *Monogr.*, 82, 205–220, 2012.

953

954 Wang, H., Prentice, I. C., Wright, I. J., Warton, D. I., Qiao, S., Xu, X., Zhou, J., Kikuzawa,
955 K., and Stenseth, N. C.: Leaf economics fundamentals explained by optimality principles, *Sci*
956 *Adv*, 9, eadd5667, 2023.

957

958 Wickham, H., Averick, M., Bryan, J., Chang, W., McGowan, L., François, R., Grolemond,
959 G., Hayes, A., Henry, L., Hester, J., Kuhn, M., Pedersen, T., Miller, E., Bache, S., Müller, K.,
960 Ooms, J., Robinson, D., Seidel, D., Spinu, V., Takahashi, K., Vaughan, D., Wilke, C., Woo,
961 K., and Yutani, H.: Welcome to the tidyverse, *J. Open Source Softw.*, 4, 1686, 2019.

962

963 Wieder, W.: RegridDED Harmonized World Soil Database v1.2,
964 <https://doi.org/10.3334/ORNLDAAAC/1247>, 2014.

965

966 Wright, I. J., Reich, P. B., Westoby, M., Ackerly, D. D., Baruch, Z., Bongers, F.,
967 Cavender-Bares, J., Chapin, T., Cornelissen, J. H. C., Diemer, M., Flexas, J., Garnier, E.,
968 Groom, P. K., Gulias, J., Hikosaka, K., Lamont, B. B., Lee, T., Lee, W., Lusk, C., Midgley, J.
969 J., Navas, M.-L., Niinemets, U., Oleksyn, J., Osada, N., Poorter, H., Poot, P., Prior, L.,
970 Pyankov, V. I., Roumet, C., Thomas, S. C., Tjoelker, M. G., Veneklaas, E. J., and Villar, R.:
971 The worldwide leaf economics spectrum, *Nature*, 428, 821–827, 2004.

972

973 Wu, H., Xiang, W., Ouyang, S., Xiao, W., Li, S., Chen, L., Lei, P., Deng, X., Zeng, Y., Zeng,
974 L., and Peng, C.: Tree growth rate and soil nutrient status determine the shift in nutrient-use
975 strategy of Chinese fir plantations along a chronosequence, *For. Ecol. Manage.*, 460, 117896,
976 2020.

977

978 Xu, M., Zhu, Y., Zhang, S., Feng, Y., Zhang, W., and Han, X.: Global scaling the leaf
979 nitrogen and phosphorus resorption of woody species: Revisiting some commonly held
980 views, *Sci. Total Environ.*, 788, 147807, 2021.

981

982 Yan, T., Zhu, J., and Yang, K.: Leaf nitrogen and phosphorus resorption of woody species in
983 response to climatic conditions and soil nutrients: a meta-analysis,
984 <https://doi.org/10.1007/s11676-017-0519-z>, 2018.

985

986 Yang, X., Post, W. M., Thornton, P. E., and Jain, A.: The distribution of soil phosphorus for
987 global biogeochemical modeling, *Biogeosciences*, 10, 2525–2537, 2013.

988

989 Yuan, Z. Y. and Chen, H. Y. H.: Global-scale patterns of nutrient resorption associated with
990 latitude, temperature and precipitation, *Glob. Ecol. Biogeogr.*, 18, 11–18, 2009.

991

992 Yuan, Z. Y. and Chen, H. Y. H.: Negative effects of fertilization on plant nutrient resorption,
993 *Ecology*, 96, 373–380, 2015.

994

995 Yuan, Z.-Y., Li, L.-H., Han, X.-G., Huang, J.-H., Jiang, G.-M., Wan, S.-Q., Zhang, W.-H., and
996 Chen, Q.-S.: Nitrogen resorption from senescing leaves in 28 plant species in a semi-arid
997 region of northern China, *J. Arid Environ.*, 63, 191–202, 2005.

998

999 Zaehle, S.: Terrestrial nitrogen-carbon cycle interactions at the global scale, *Philos. Trans. R.*
1000 *Soc. Lond. B Biol. Sci.*, 368, 20130125, 2013.

1001

1002 Zaehle, S., Medlyn, B. E., De Kauwe, M. G., Walker, A. P., Dietze, M. C., Hickler, T., Luo,
1003 Y., Wang, Y.-P., El-Masri, B., Thornton, P., Jain, A., Wang, S., Warlind, D., Weng, E., Parton,
1004 W., Iversen, C. M., Gallet-Budynek, A., McCarthy, H., Finzi, A., Hanson, P. J., Prentice, I.
1005 C., Oren, R., and Norby, R. J.: Evaluation of 11 terrestrial carbon-nitrogen cycle models
1006 against observations from two temperate Free-Air CO₂ Enrichment studies, *New Phytol.*,
1007 202, 803–822, 2014.

1008

1009 Zhang, M., Luo, Y., Meng, Q., and Han, W.: Correction of leaf nutrient resorption efficiency
1010 on the mass basis, *J Plant Ecol*, 15, 1125–1132, 2022.

1011

1012

1013

1014

1015

1016

1017

1018

1019

1020

1021

1022 Appendix A - Sensitivity study of the importance of MLCF

1023 We assembled the global dataset from the gap-filled version of TRY Plant Trait database
1024 (<https://www.try-db.org>, Kattge et al., 2020, version 5.0) containing field measurements of
1025 paired leaf and litter mass-based tissue N and P concentrations ($N_{\text{mass, leaf}}$, $P_{\text{mass, leaf}}$, $N_{\text{mass, litter}}$,
1026 $P_{\text{mass, litter}}$) to derive the fractional nutrient resorption (described in Methods Sect. 2.1).

1027 In order to understand the importance of considering MLCF in the formula to derive reliable
1028 nutrient resorption values, we compared four sub datasets from the final global dataset:

1029 (a) we derived nutrient resorption from nutrient resorption database, in which MLCF was
1030 calculated directly from leaf dry mass or leaf mass loss measurements;

1031 (b) the second dataset we derived nutrient resorption from nutrient resorption database as
1032 well, but we filled the missing values of MLCF using the mean for each plant functional type
1033 (PFT): 0.712 for deciduous, 0.766 for evergreen, 0.69 for conifers, and 0.75 for woody lianas,
1034 respectively.

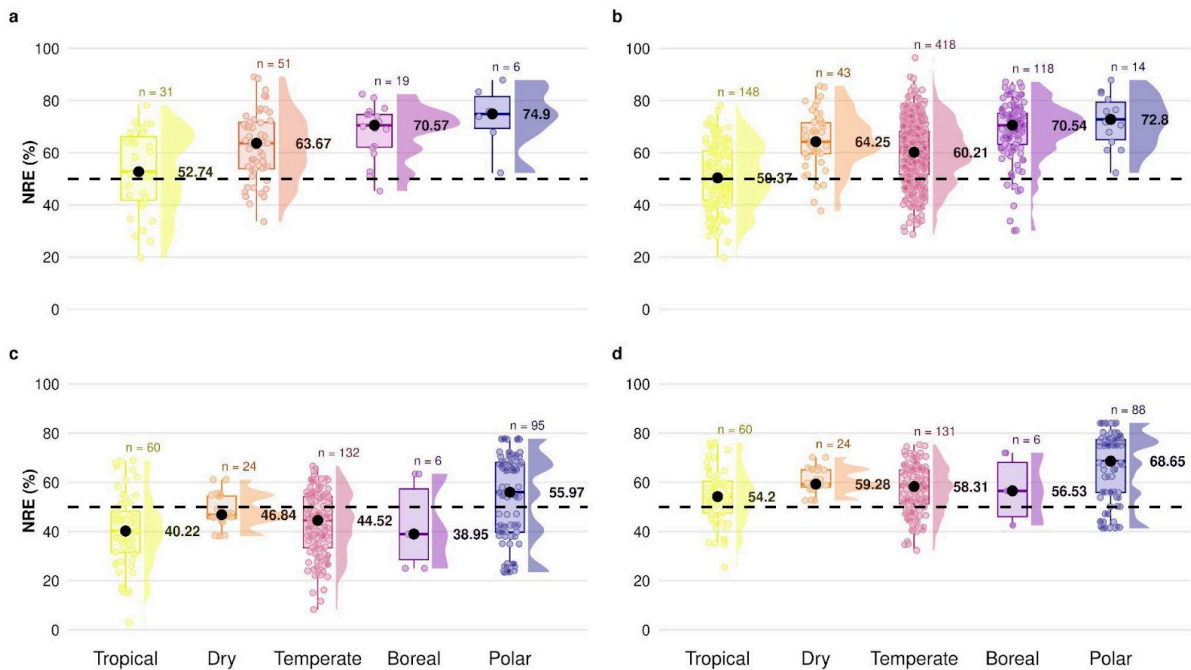
1035 (c) the third dataset we derived nutrient resorption using leaf nutrient and litter data from
1036 TRY traits, in which we did not include MLCF in the formula, calculated as:

$$1037 \quad NuRE = \left(1 - \frac{Nu_{\text{senesced}}}{Nu_{\text{green}}}\right) \times 100 \quad (2)$$

1038 (d) the fourth dataset we derived nutrient resorption using leaf nutrient and litter data from
1039 TRY, but here we filled MLCF with the mean per PFT calculated before, in which we
1040 associated these means with leaf habit, leaf type and growth form information. For that, trees
1041 with needle evergreen leaves received conifers MLCF, deciduous trees/shrubs received
1042 deciduous woody MLCF, and evergreen trees/shrubs received evergreen woody MLCF,
1043 respectively.

1044 Figure A1 shows nitrogen resorption efficiency (NRE) between different climate zones,
1045 where we can see underestimated values of resorption only when we do not consider MLCF
1046 in the formula (Fig. A1c), with values around or lower 50% of N resorption. We can see more
1047 reliable resorption values around 60% when considering MLCF in the formula (Fig. A1a A1b
1048 A1d). When applying the mean of MLCF for the table deriving NRE from TRY traits (Fig.
1049 A1d), we are able to reproduce a similar pattern compared to the resorption database
1050 imported from TRY (Fig. A1a). Figure A2 shows the distribution of NRE for each subset
1051 described before, where we can see a clear difference in data distribution only when we do

1052 not consider MLCF in the formula (Fig. A2c). For our final dataset, we then considered
 1053 together the dataset (b) and (d), in which are the most reliable data for nutrient resorption as it
 1054 is providing more data points for resorption and considers MLCF in the formula.



1055

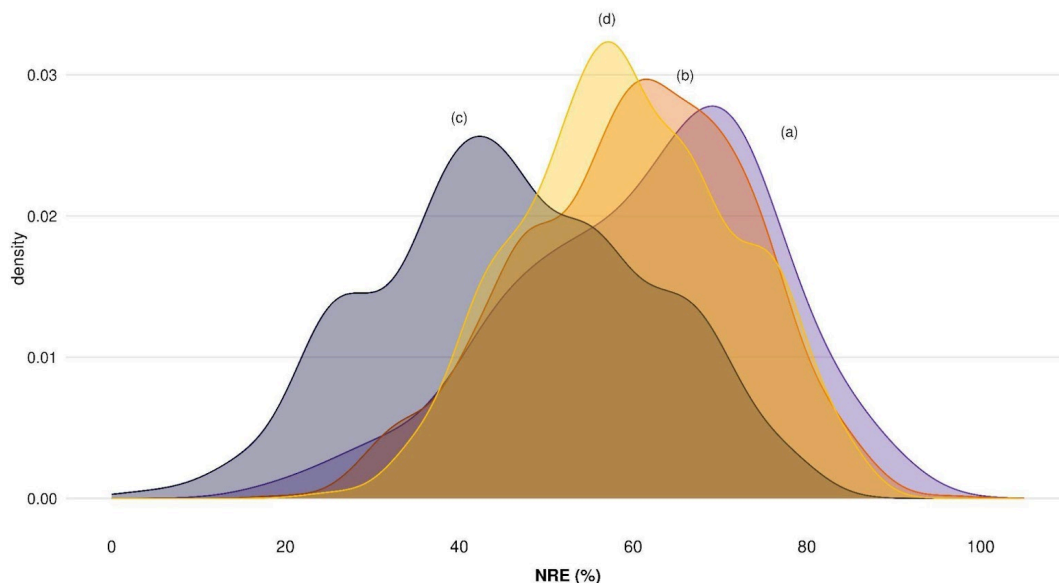
1056

1057 **Figure A1:** Difference in nitrogen resorption efficiency (NRE %) among climate gradients from tropical to
 1058 polar zones based on the Köppen climate classification, comparing four sub datasets to understand the
 1059 importance of mass loss correction factor (MLCF) in the formula to derive nutrient resorption values: **(a)**
 1060 nutrient resorption values derived directly from nutrient resorption dataset, with MLCF calculated from leaf dry
 1061 mass or leaf mass loss measurements; **(b)** nutrient resorption values derived directly from nutrient resorption
 1062 dataset, but with missing MLCF filled by the mean for each plant functional type (PFT); **(c)** nutrient resorption
 1063 values derived from TRY traits with no MLCF in the formula; **(d)** nutrient resorption values derived from TRY
 1064 traits, but with missing MLCF filled by the mean for each PFT. Boxplots depict median (black dots),
 1065 interquartile range and outliers, indicating data spread and variability. The side distributions show the overall
 1066 data distribution for each climate zone. The dashed line indicates the overall mean NRE of 50% used in most
 1067 land surface models. ‘n’ represents the number of observations per climate zone.

1068

1069

1070



1071

1072 **Figure A2:** Distribution of nitrogen resorption efficiency (NRE %) comparing four sub datasets to understand
 1073 the importance of mass loss correction factor (MLCF) in the formula to derive nutrient resorption values: **(a)**
 1074 nutrient resorption values derived directly from nutrient resorption dataset, with MLCF calculated from leaf dry
 1075 mass or leaf mass loss measurements; **(b)** nutrient resorption values derived directly from nutrient resorption
 1076 dataset, but with missing MLCF filled by the mean for each plant functional type (PFT); **(c)** nutrient resorption
 1077 values derived from TRY traits with no MLCF in the formula; **(d)** nutrient resorption values derived from TRY
 1078 traits, but with missing MLCF filled by the mean for each PFT.

1079

1080 Appendix B - Global patterns of nutrient resorption efficiency for N and P 1081 by PFTs and climate zones

1082 **Table B1** | Summary of nitrogen resorption efficiency (NRE; %) and phosphorus resorption efficiency (PRE; %)
 1083 in different climate zones. For each relationship, the number of observations (N), minimum (Min), maximum
 1084 (Max), median, and standard deviation (SD) were reported. Letters in Significance show the statistical
 1085 comparison between each climate zone.

Resorption (%)	Climate zone	N	Min	Max	Median	SD	Significance
NRE	Tropical	178	19.77	78.23	52.46	12.15	a
	Dry	65	37.17	85.48	61.66	9.72	bc
	Temperate	507	28.77	89.11	59.18	11.06	c
	Boreal	102	29.64	86.72	69.03	11.0	b
	Polar	102	41.42	87.89	69.62	12.84	b
PRE	Tropical	100	27.65	87.23	61.7	12.84	ns
	Dry	5	42.55	72.31	66.09	11.47	ns
	Temperate	273	29.14	95.11	57.80	13.65	a
	Boreal	57	35.92	88.88	67.36	13.65	b
	Polar	12	52.16	83.58	68.02	8.84	ns

1086

1087 **Table B2** | Summary of nitrogen resorption efficiency (NRE; %) and phosphorus resorption efficiency (PRE; %) 1088 in different plant functional types (PFTs). For each relationship, the number of observations (N), minimum 1089 (Min), maximum (Max), median, p value and standard deviation (SD) were reported. ‘p-value’ < 0.05 indicates 1090 statistical significance.

Resorption (%)	PFT	N	Min	Max	Median	p value	SD
NRE	Deciduous	400	29.64	89.11	65.27		12.48
	Evergreens	551	19.77	87.89	57.96	<0.001	11.45
	Broad-leaves	841	19.77	89.11	59.8		12.53
	Needle-leaves	103	40.19	87.89	61.84	0.05	9.97
	Shrubs	230	30.13	85.48	63.17		12.48
	Trees	724	19.77	89.11	59.27	<0.001	12.17
PRE	Deciduous	220	29.22	95.78	60.04		12.86
	Evergreens	231	27.65	91.78	61.7	0.46	14.41
	Broad-leaves	404	27.65	95.11	59.64		13.50
	Needle-leaves	45	51.35	88.88	72.2	<0.001	9.23
	Shrubs	59	32.97	87.23	64.4		13.50
	Trees	395	27.65	95.11	61.1	0.89	13.67

1091

1092

1093 **Table B3** | Summary of Nitrogen resorption efficiency (NRE; %) and Phosphorus resorption efficiency (PRE; 1094 %) in different plant functional types (PFT) separated in different climate zones. For each relationship, the 1095 number of observations (N), minimum (Min), maximum (Max), median, and standard deviation (SD) were 1096 reported. Letters in Significance show the statistical comparison between each climate zone.

NRE							
PFT	Climate zones	N	Min	Max	Median	SD	Significance
Deciduous	Tropical	31	31.97	71.80	52.53	11.64	a
	Dry	31	37.17	85.48	65.95	11.68	b
	Temperate	216	31.95	89.11	62.39	11.84	cb
	Boreal	61	29.64	86.72	68.28	11.17	db
	Polar	61	47.15	84.16	75.60	9.99	e
Evergreens	Tropical	147	19.77	78.23	52.43	12.28	a
	Dry	34	40.97	79.57	60.42	7.06	bc
	Temperate	288	28.77	81.56	58.40	9.93	cd
	Boreal	41	30.13	82.44	70.57	10.87	b
	Polar	41	41.42	87.89	56.03	13.44	d
Broad-leaves	Tropical	174	19.77	78.23	52.46	12.15	a
	Dry	63	37.17	85.48	61.66	9.42	bc
	Temperate	453	28.77	89.11	59.18	11.36	c
	Boreal	69	29.64	86.72	68.28	12.13	b

	Polar	82	41.42	84.16	75.10	12.34	b
Needle-leaves	Tropical	1	65.25	65.25	65.25	-	ns
	Dry	2	46.60	79.65	63.13	23.37	ns
	Temperate	47	40.19	81.56	58.80	7.45	a
	Boreal	33	51.02	82.44	71.52	7.33	b
	Polar	20	46.76	87.89	56.03	11.58	a
Shrubs	Tropical	21	33.81	74.33	59.60	11.45	a
	Dry	33	37.17	85.48	63.72	12.08	ns
	Temperate	77	31.29	80.96	59.16	10.63	a
	Boreal	27	30.13	85.15	65.77	13.66	ns
	Polar	72	41.42	84.16	71.16	11.92	b
Trees	Tropical	157	19.77	78.23	52.35	12.18	a
	Dry	32	47.10	76.26	60.08	6.59	bc
	Temperate	430	28.77	89.11	59.18	11.13	c
	Boreal	75	29.64	86.11	70.05	9.49	b
	Polar	30	46.76	87.89	68.44	14.89	bc

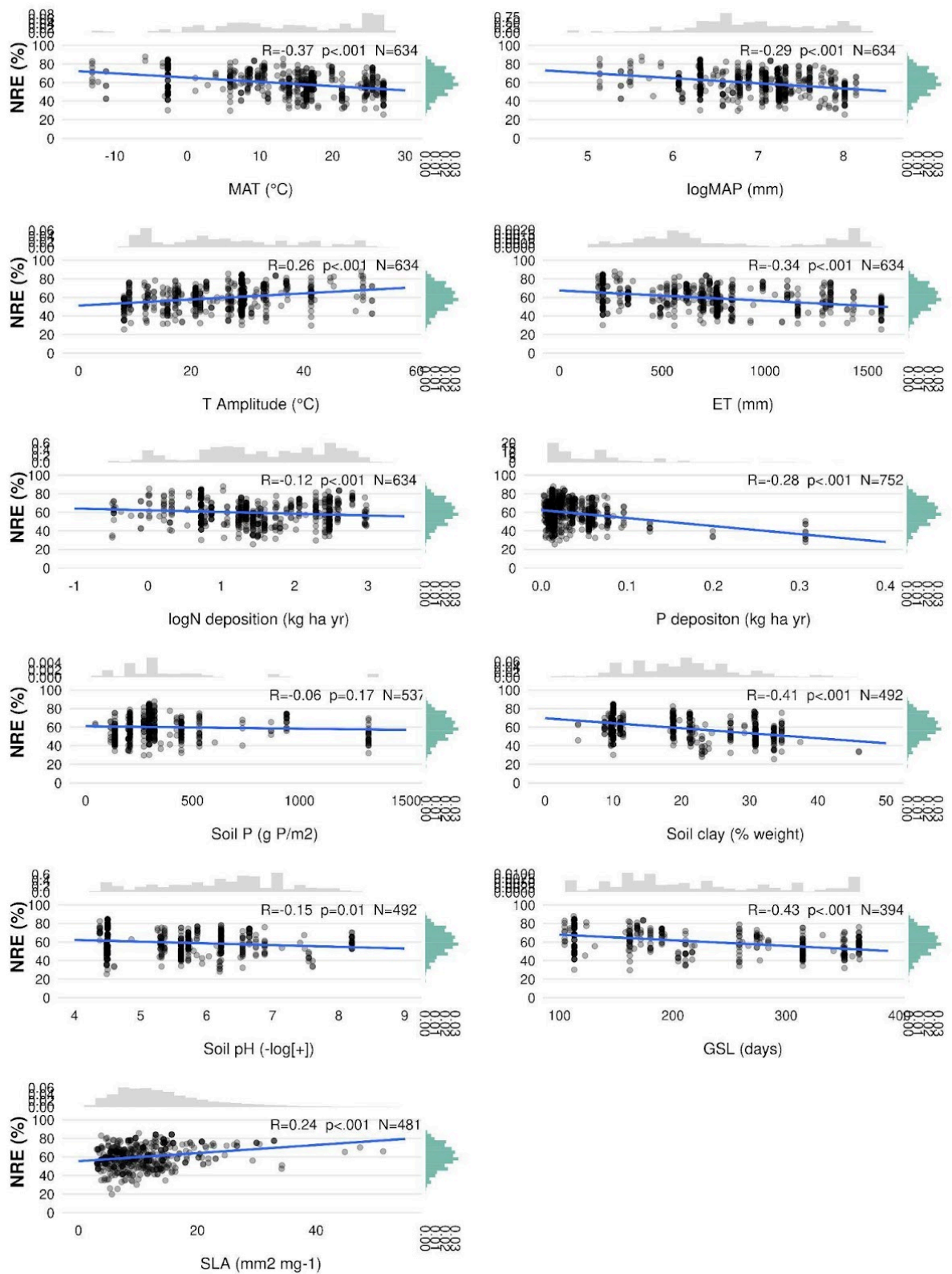
PRE

PFT	Climate zones	N	Min	Max	Median	SD	Significance
Deciduous	Tropical	25	35.92	76.26	64.40	13.14	ns
	Dry	4	64.40	72.31	66.29	3.44	ns
	Temperate	145	29.22	95.11	59.95	13.32	ns
	Boreal	33	35.92	84.33	59.31	12.18	ns
	Polar	6	59.31	71.52	64.51	4.90	ns
Evergreens	Tropical	75	27.65	87.23	61.70	12.81	a
	Dry	1	42.55	42.55	42.55	-	ns
	Temperate	125	29.14	91.78	57.44	13.85	a
	Boreal	24	61.38	88.88	79.26	7.58	b
	Polar	6	52.16	83.58	73.73	11.03	ns
Broad-leaves	Tropical	97	27.65	87.23	61.70	12.98	ns
	Dry	5	42.55	72.31	66.10	11.47	ns
	Temperate	249	29.14	95.11	57.28	13.93	ns
	Boreal	36	35.92	84.33	60.14	11.92	ns
	Polar	10	52.16	83.58	68.03	9.63	ns
Needle-leaves	Temperate	22	51.35	82.62	65.25	7.06	a
	Boreal	21	61.38	88.88	80.14	7.22	b
	Polar	2	67.02	73.00	70.01	4.22	ns
Shrubs	Tropical	14	47.85	79.97	61.95	10.39	ns
	Dry	3	42.55	66.09	64.40	13.13	ns
	Temperate	20	32.97	87.23	52.72	17.36	ns
	Boreal	13	46.60	82.20	67.17	10.70	ns
	Polar	9	52.16	83.58	71.52	10.0	ns
Trees	Tropical	86	27.65	87.23	61.70	13.24	ns
	Dry	2	66.49	72.31	69.40	4.11	ns

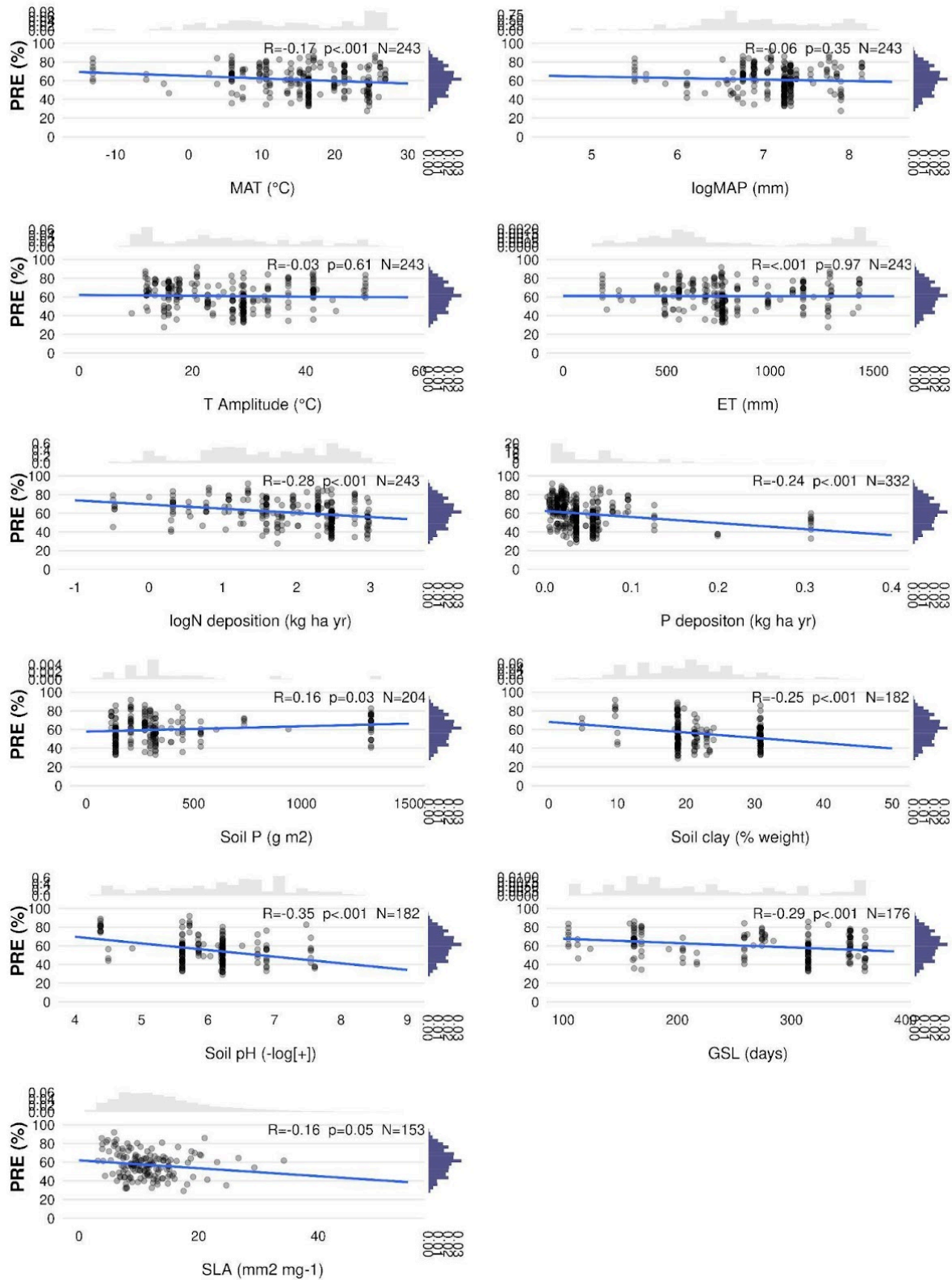
Temperate	253	29.14	95.11	58.78	13.35	a
Boreal	44	35.92	88.88	67.78	14.48	b
Polar	3	61.11	68.68	67.03	3.97	ns

1097
1098
1099
1100
1101
1102
1103
1104
1105
1106
1107
1108
1109
1110
1111
1112
1113
1114
1115
1116
1117
1118
1119
1120
1121
1122
1123
1124
1125
1126
1127
1128
1129
1130
1131
1132
1133

1134 Appendix C - Linear regressions of nutrient resorption with environmental
 1135 and biological factors



1136

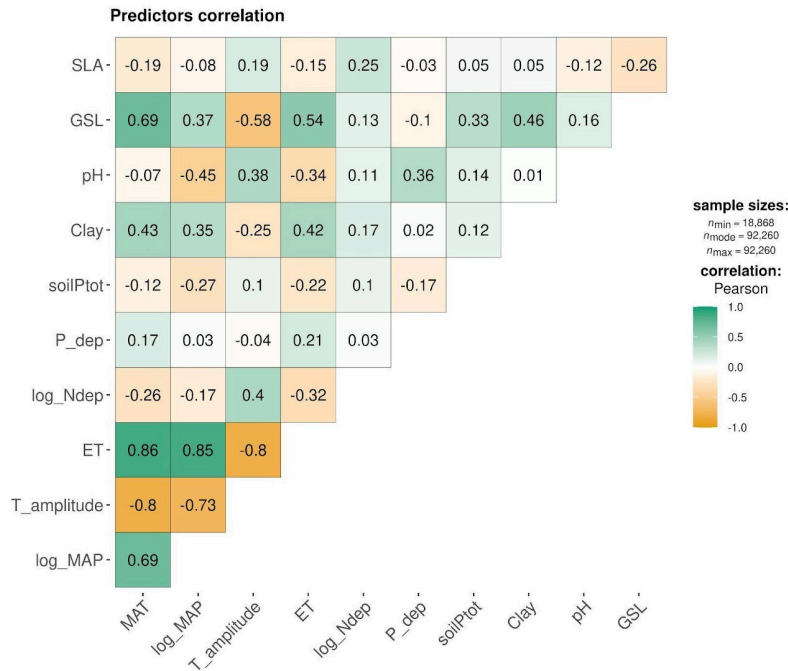


1137

1138 **Figure C1.** Linear regression of nitrogen resorption efficiency (NRE; %) and phosphorus resorption efficiency
 1139 (PRE; %) with all possible predictor variables. Environmental predictors: Mean Annual Temperature (MAT),
 1140 Mean Annual Precipitation (MAP), Evapotranspiration (ET), Temperature amplitude (T amplitude), Nitrogen
 1141 deposition (N deposition), Phosphorus deposition (P deposition), total soil P (soil P) soil clay fraction (Soil

1142 Clay), soil pH. Biological predictors: Growing Season Length (GSL), Specific Leaf Area (SLA). R: Pearson
 1143 correlation; $p < 0.05$ indicates statistical significance; N: number of observations. The distribution on the right
 1144 of the correlation represents the overall distribution of NRE and PRE values for each predictor.

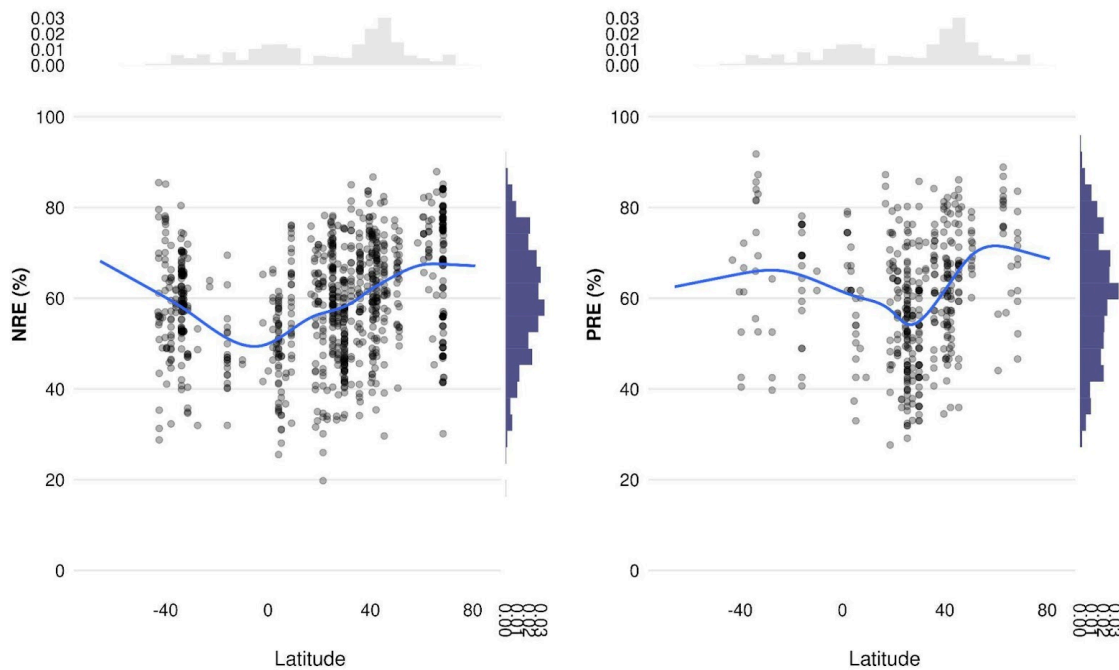
1145
 1146
 1147



1148

X = non-significant at $p < 0.05$ (Adjustment: Holm)

1149 **Figure C2:** Multiple Pearson correlation matrix between all predictors. The color scale indicates the strength of
 1150 the correlations, with green representing positive correlations and orange representing negative correlations,
 1151 with non-significant correlations at $p < 0.05$ indicated by 'X'. Mean Annual Temperature (MAT); Mean Annual
 1152 Precipitation (MAP); Evapotranspiration (ET); Temperature amplitude (T amplitude); Nitrogen deposition (N
 1153 deposition); Phosphorus deposition (P deposition); total soil P (soilPtot); soil clay fraction (Clay); soil pH;
 1154 Growing Season Length (GSL); Specific Leaf Area (SLA).

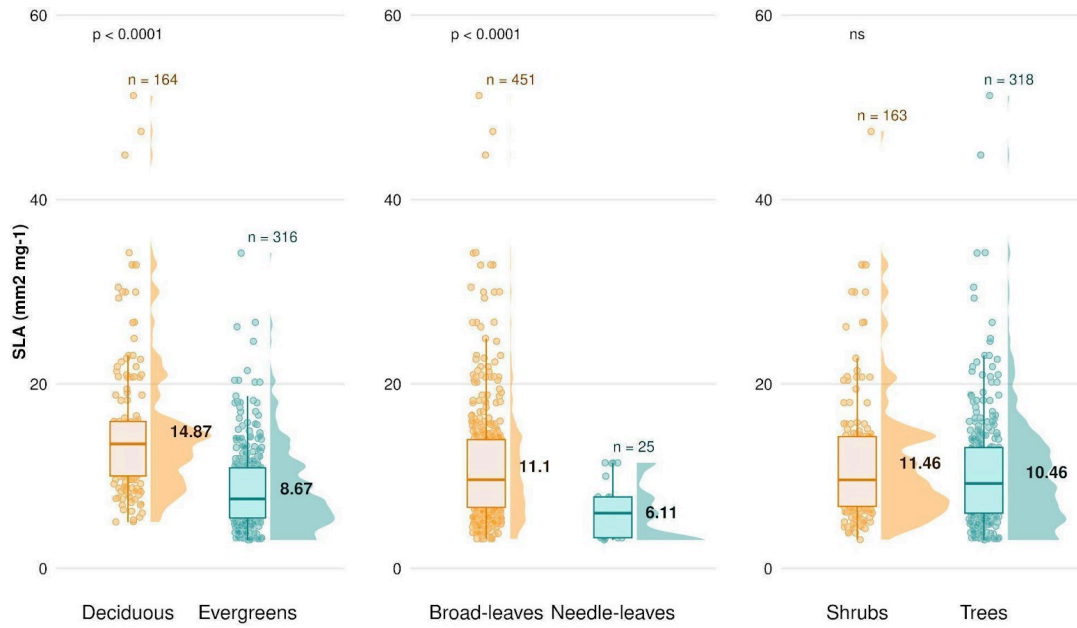


1155

1156 **Figure C3:** Relationship between nitrogen resorption efficiency (NRE %) and phosphorus resorption efficiency
 1157 (PRE %) with latitude. The scatter plots display individual observations, with the blue lines representing the
 1158 smoothed regression curves indicating trends in NRE and PRE across latitudes. Histograms on the top and right
 1159 margins show the density distributions of latitude and resorption efficiencies, respectively. This visualization
 1160 highlights the variation in nutrient resorption efficiencies across different latitudinal gradients.

1161

1162 PFTs do not appear in the correlation matrix shown in Fig. C1 and C2, as it is a categorical
 1163 variable. However, we explore the implication of SLA on nutrient resorption based on the
 1164 strong and known relationship between SLA and PFTs in our dataset (Fig. C4), which derives
 1165 from the leaf economics spectrum (LES) theory.



1166

1167 **Figure C4:** Difference in the specific leaf area (SLA; mm² mg⁻¹) between plant functional types (PFTs) on a
 1168 global scale, comparing deciduous vs. evergreens, broadleaved species vs. needle leaves, and shrubs vs. trees.
 1169 Boxplots depict median, interquartile range and outliers, indicating data spread and variability. The side
 1170 distributions show the overall data distribution for each PFT. ‘n’ represents the number of observations, ‘p’
 1171 values indicate the significance of differences in SLA between PFTs, and ‘ns’ indicates no significant difference.